Isolation and Identification of a Novel Putative WT1-Interacting Protein

A thesis submitted to the Faculty of Graduate Studies and Research
in partial fulfillment of the requirement
of the degree of Masters of Science.

By

Shelly Lwu

Department of Biochemistry
McGill University, Montreal
August 2000

ABSTRACT

The *WT1* gene encodes a transcription factor that is involved in the etiology of the nephroblastoma, Wilms' Tumor, and its associated diseases. Protein-protein interactions have been shown to alter the transcription regulatory functions of WT1 and implicate WT1 in the post-transcriptional event, splicing. Modulation of WT1 activity by its interacting partner and vice versa can extend the functional capacity of both proteins. A new potential WT1-interacting protein, Bone Marrow Zinc Finger 2 (BMZF2 or ZNF255), was isolated by affinity chromatography from HeLa cell nuclear extracts and subsequently identified by mass spectrometry analysis. Amino acid sequence analysis of BMZF2 suggests that it is a potential transcription factor with DNA-binding abilities. GST pulldown experiments indicate that BMZF2 binds the zinc finger region of the WT1 (–KTS) isoform in vitro. Because BMZF2 targets the WT1 (–KTS) zinc finger domain, it may be capable of influencing WT1's transcriptional regulatory functions. The expression patterns of BMZF2 and WT1 suggest that they may be important to the regulation of mammalian development and hematopoiesis.

ACKNOWLEDGEMENT

I would like to thank Dr. Jerry Pelletier for his supervision and guidance during my studies. It is my privilege to have been able to work under him and learn from him.

I would also like to express my sincerest appreciation for all the support and guidance that the members of my lab have given me. Much thanks to the wonderful and fun-loving group of people that I work with now: Maria Discenza, Tae Ho Lee, Lee Lee Chu, Jennifer Michel, Isabelle Harvey, Eun-Hee Park, and Sofia Moraitis; and to the past members of the lab: Manjula Das, Jung Ho Kim, Peter Moffett, Majid Ghahremani, and Mohammad Dehbi. I will always cherish their friendship. A special thanks to Isabelle who translated the abstract into French for me.

I would like to thank my family for always believing in me. I am forever indebted to my boyfriend, Roberto Lin, for his unfailing support and encouragement, as well as assistance with the figures.

Credit is due to Dr. Brian Cox of Borealis Biosciences Inc. (Toronto, Canada) who generated the mass spectrometry data for this thesis.

Table of Contents

Figures

RESUME

Le gène WT1 encode un facteur de transcription impliqué dans l'étiologie du neuroblastome, de la tumeur de Wilms ainsi que de ses affections associées. L'interaction de WT1 avec d'autres protéines altèrent ses fonctions de régulation de transcription et l'impliquent dans l'événement post-transcriptionnel appelé épissage. La modulation de l'activité de WT1 par ses partenaires d'interaction et vice versa peut étendre la capacité fonctionnelle des deux protéines. Une nouvelle protéine potentiellement associée à WT1, "Doigt de zinc 2 de moelle-épinière" (BMZF2 ou ZNF255), a été isolée par chromatographie d'affinité à partir d'extraits nucléaires de cellules Hela et par la suite identifiée par analyse par spectroscopie de masse. L'analyse de la séquence d'acides aminés de BMZF2 suggère que c'est un facteur de transcription potentiel avec des capacités à coupler l'ADN. Les essais de co-précipitation par la GST indiquent que BMZF2 reconnaît in vivo la région du doigt de zinc de l'isoforme de WT1 (-KTS). Parce que BMZF2 reconnaît le domaine du doigt de zinc de WT1 (-KTS), il peut être capable d'influencer les fonctions de régulation de la transcription de WT1. Les patrons d'expression de BMZF2 et de WT1 suggèrent qu'ils peuvent être importants pour la régulation du développement des mammifères et de l'hématopoïèse.

INTRODUCTION

Wilms' Tumor and the Wilms' Tumor 1 Gene

Wilms' tumor or nephroblastoma is a pediatric kidney cancer first described by Max Wilms in 1899 (1). It is one of the most common childhood malignancies found in children under age 5, occurring with a frequency of 1 in 10,000 (2,3). The tumor is of embryonic origin and is derived from the metanephric blastemal tissues of the developing kidney that failed to undergo the normal maturation process (4). Urogenital abnormalities represent the major clinical features of Wilms' Tumor and are also included in the clinical spectrum of its related syndromes, Denys-Drash and WAGR (Wilms' tumor, aniridia, genitourinary malformation, and mental retardation) (5).

Cytogenetic and molecular studies have shown that several chromosomal regions may be involved in the development of Wilms' Tumor, however, only the Wilms' Tumor 1 gene (*WT1*), located at chromosome 11p13, has been proven to play a role in the etiology of this tumor (6). In humans, heterozygous mutations of the *WT1* gene predispose to Wilms' Tumors (7-9). Transfection of wild-type *WT1* into a Wilms' Tumor cell line with aberrant endogenous *WT1* transcripts results in tumor growth suppression (10). The essential role of *WT1* in urogenital development is further underscored by the failure of *WT1*-null mice to develop kidneys and gonads (11). Wilms' Tumor and the *WT1* gene, therefore, provide an excellent model for studying the relationship between cancer and development.

WT1 and Kidney Development

The development of the kidney depends on the interactions between two different tissues: the ureteric epithelium, which is derived from the Wolffian duct, and the surrounding metanephric mesenchyme (1). The formation of the nephrons, the functional subunits of the kidney, occurs through a sequence of inductive and reciprocal interactions between these two tissues. The initial budding of the ureter depends on the inductive signal from the surrounding mesenchyme. As the ureter branches, the mesenchyme condenses around the tip of the branching ureter and forms the blastema around the ureteric bud. The blastema develops into the renal vesicle and matures in association with the ureter, which elongates and folds into comma- and S-shaped bodies. The epithelial cells on the S-shaped body eventually form the proximal tubules, the distal tubules, and the glomerulus of the mature nephron. The condensation of the metanephric mesenchyme depends on the signals from the ureter and therefore, the signals from the mesenchyme and the ureter must be complemented by receptors in the responding tissues. Similar mesenchyme-epithelium interactions are also observed during the development of many other organs (12).

WT1 appears to function at three different stages of kidney development: the onset of nephrogenesis, the progression of nephrogenesis, and the maintenance of normal podocyte function (1). *WT1* expression levels are low in the uninduced mesenchyme and absent in its reciprocally induced tissue, the ureter epithelium (13). *WT1* expression increases as the mesenchyme condenses into the comma- and S-shaped bodies. Further differentiation is coupled with the downregulation of *WT1* expression, while in the

mature nephron, *WT1* is expressed only in the podocytes, a highly specialized layer of epithelial cells that line the blood vessels in the glomerulus.

WT1 is essential for the development of the ureteric bud. In the *WT1*-null mouse, the ureteric bud is absent although normal mesenchymal cells are observed at day 11.5 of embryonic development (11). Apoptosis of the mesenchyme then occurs and half a day later, the mesenchymal cells disappear. The absence of the ureteric bud in the *WT1*-null embryos suggests that *WT1* is either directly or indirectly responsible for the generation of the signal from the mesenchyme that is perceived by the ureter. *WT1* is also responsible for the competence of the mesenchyme to respond to signals from the ureter and condense. When the mesenchyme from the wild-type and the *WT1*-knockout embryos are cultured next to the spinal cord, a strong inducer of tubular differentiation, the wild-type mesenchyme differentiates to form tubular structures; however, the mesenchyme from the *WT1*-knockout embryos did not (11). This demonstrates that *WT1* has a dual role during the formation and differentiation of the kidney.

WT1 Expression Pattern and Associated Diseases

The expression pattern of the *WT1* gene indicates that its function is not restricted to the kidney only. *WT1* also plays a role in the development and homeostasis of other tissues. The products of *WT1* seem to possess diverse functions and are implicated in various cellular processes, such as, proliferation, differentiation, and apoptosis. There is also evidence to suggest that some functions of the WT1 protein are cell-type specific.

In situ hybridization on sections of chicken, mouse, and human embryos showed that *WT1* is expressed during embryonic development (13,14). In addition to *WT1*'s expression in the glomerular precursor cells of the fetal kidney, *WT1* is also expressed in the stromal cells of the gonads and spleen; mesothelial cells lining the heart, diaphragm, and peritoneum; differentiating body wall musculature; and pocket regions in the brain and spinal cord (15,16).

WT1 plays a common role in the development of these structures and this is illustrated by its absence or aberrant expression and the associated disease phenotype. *WT1*-null mice show a lack of kidney, gonad, and mesothelial development (11). Dominant heterozygous mutations in *WT1* cause nearly all cases of the Denys-Drash syndrome, a rare developmental disorder of the genito-urinary system (8). Heterozygous deletions of *WT1* are found in WAGR patients who also often exhibit urogenital abnormalities (9). Mutations in a *WT1* intron, affecting alternative splice site selection, are associated with Frasier syndrome, a rare disease defined by male pseudo-hermaphroditism and progressive glomerulopathy (17,18). This points to functional

differences between various splice forms of the WT1 protein. *WT1* mutations also occur in rare mesotheliomas (19). Desmoplastic Small Round Cell Tumor, a mesothelial-derived cancer, results from a chromosomal translocation which fuses the putative transactivation domain of the Ewing Sarcoma gene to the C-terminus of WT1 (20). While *WT1* normally acts as a recessive tumor-suppressor gene, it acquires the properties of a dominant oncogene when fused to the specific amino terminal domain of the EWS gene. *WT1* mutations are also found in 4 of 36 acute leukemias, where the small insertions are predicted to produce truncated WT1 proteins (21). The loss of heterozyosity of the WT1 gene has been found to correlate with in situ and invasive stages of breast carcinoma (22), and altered proportions of WT1 splice variants have also been detected in other breast tumors (23).

WT1 Gene and Protein Structure

The *WT1* gene is localized to the human chromosome 11p13 region (6). The gene is approximately 50 kilobases (kb) in length and contains 10 exons, which is transcribed and processed into a 3 kb mRNA species (24) **(Figure 1)**. The WT1 protein is a typical transcription factor. It contains a glutamine/proline-rich N-terminus, transcription activation and repression domains, nuclear-localization signals, and four Kruppel-like Cys_2/His_2 zinc fingers at the C-terminus. The four zinc fingers, amino acids 307 to 429, that constitute the DNA-binding region, share a homology of 67% with the zinc fingers of the Early Growth Response-1 (EGR-1) family members (25,26). Amino acids 226 to 254 contain partial heptad repeats of leucine residues and this potential leucine zipper

Figure 1:

Structure of (a) *WT1* gene and (b) WT1 protein. WT1 is encoded by ten exons. Three translational start sites are possible for the *WT1* mRNA: a standard methionine; a second in-frame downstream AUG that is an internal translation initiation site, and an upstream CUG (leucine), which adds 68 N-terminal residues onto the WT1 protein. Alternative splicing of exon 5 and alternative usage of two different splice-donor sites at the 3' end of exon 9 produce four different splice forms. The inclusion of splice I (exon 5) leads to an insertion of 17 amino acid residues. The splice II sequence at the 3' end of exon 9 consists of the tripeptide, KTS, which is inserted between zinc fingers III and IV. A Pro/Gln-rich region, which is almost identical to the self-association domain, as well as a repression and an activation domain, are indicated. Some of WT1's C-terminal nuclear localization signals have also been indicated. A predicted RNA-binding motif resides in the N-terminus.

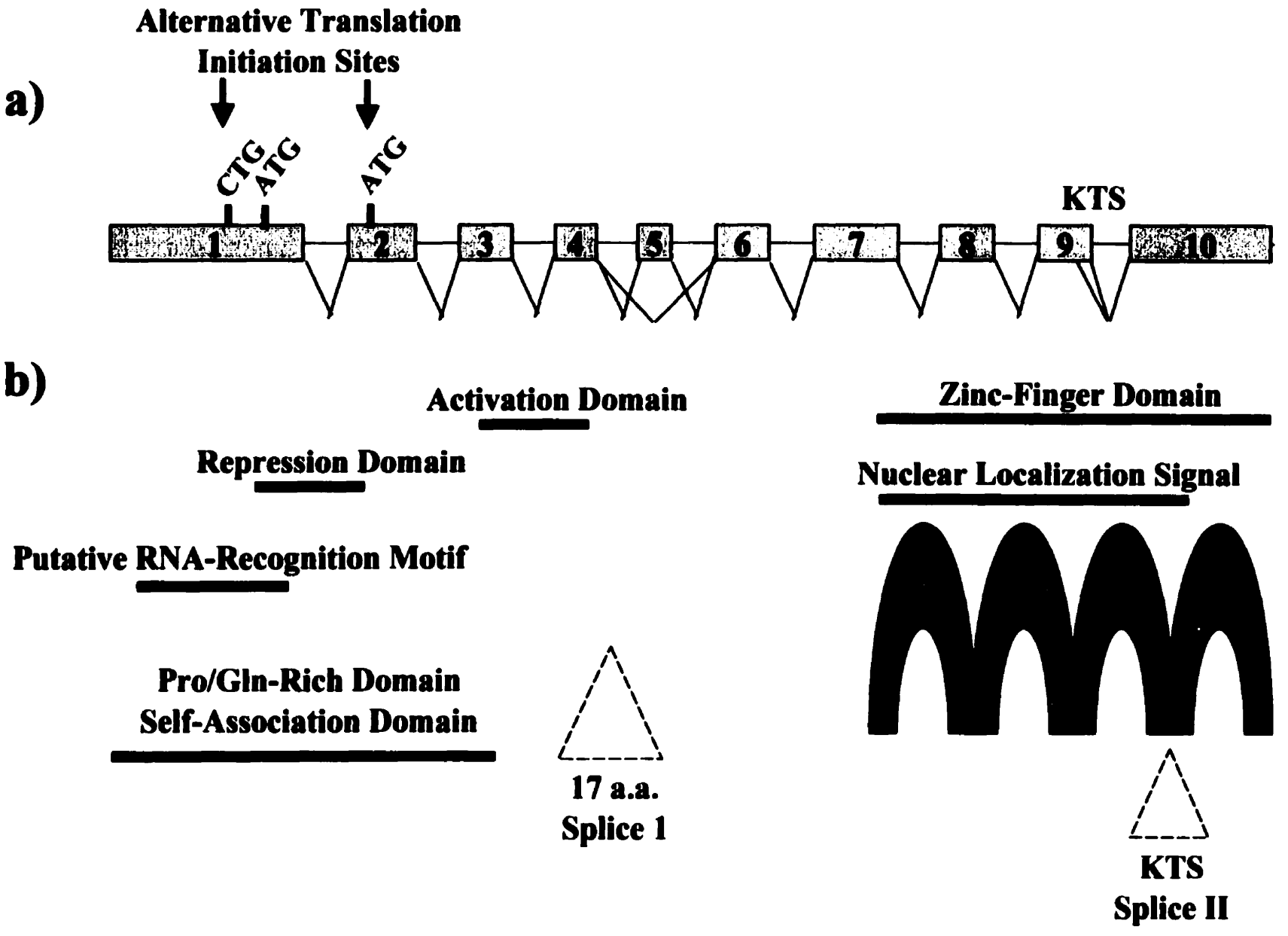
a)
Alternative Translation
Initiation Sites
CTG
ATG
ATG
KTS
1
2
3
4
5
6
7
8
9
10
b)
Activation Domain
Zinc-Finger Domain
Repression Domain
Nuclear Localization Signal
Putative RNA-Recognition Motif
Pro/Gln-Rich Domain
Self-Association Domain
17 a.a.
Splice 1
KTS
Splice II

may mediate protein-protein interactions (27). The N-terminal 180 amino acids mediate self-association, which has been demonstrated both in vitro and in vivo (28,29). This self-association domain partially overlaps with amino acids 85 to 124 and 181 to 250, domains that can autonomously repress or activate transcription respectively, in conjunction with the DNA-binding domain (30).

The *WT1* gene encodes multiple protein isoforms. At least 32 isoforms are possible as a result of alternative splicing events, an RNA editing event, and alternative upstream translation start sites. Three translational start sites are possible: a standard methionine; a second in-frame downstream AUG that is an internal translation initiation site (31); and an upstream CUG (leucine), which adds 68 N-terminal residues onto the WT1 protein (32). The consequences of the alternative translation start sites are unclear. The *WT1* mRNA is edited in the adult but not in neonatal rat kidneys and in the human testis; a thymidine to cytosine change in exon 6 leads to a leucine to proline change in the amino acid sequence (33). WT1 proteins with this change repress transcription from the *EGR-1* promoter 25 to 30% less efficiently than the wild-type version. Two alternative RNA splice sites generate four WT1 isoforms (34) that range in molecular mass from 52 to 54 kilodaltons (kDa) (35). Splice site one results in either the inclusion or exclusion of exon 5 of the gene, which encodes 17 amino acids lying just N-terminal of the four zinc fingers. Splice site two involves an alternative splice donor site at the exon 9 boundary which results in the presence or absence of a three-amino acid insert, lysine-threonine-serine (KTS), between zinc fingers 3 and 4. The +KTS isoform exists in the cell in higher abundance than the –KTS isoform, at a ratio of ~2:1 (34).

DNA and RNA Binding by WT1

All four WT1 alternative splice forms can bind DNA via their zinc finger regions, albeit with different affinities and specificities, and thereby modulate the transcriptional activity of their target genes (26). The –KTS isoform seems to exhibit greater DNA binding abilities than the +KTS isoform. WT1 (-KTS) binds the $^{5'}$GCGGGGGCG$^{3'}$ sequence, commonly denoted as the EGR-1 consensus sequence for its role as a target sequence to the EGR-1 gene product. WT1 also binds a TC-rich motif with equal affinity, $^{5'}$(TCC)$_4$TCTCC$^{3'}$ (36). Promoter analysis of candidate WT1 target genes and systematic searches for WT1 binding sites have produced variations of the EGR-1 consensus motif and the TC-rich motif (1). WT1 also shows high affinity for heteroduplex DNA (37), which is usually a product of bubble formation during replication or transcription, occurring when the double stranded DNA melts. This DNA structural requirement is interesting, as a previous report showed that WT1 could inhibit DNA replication (38).

WT1 can also bind RNA in vitro. The first zinc finger of WT1 has been shown to bind a sequence in exon 2 of the insulin-like growth factor 2 mRNA (39). Three unrelated candidate RNA target sequences were identified by the SELEX (Systematic Evolution of Ligands by Exponential Enrichment) method and shown to bind zinc fingers 2 to 4 of WT1 (40). The WT1 (+KTS) isoform exhibits a reduced affinity for these RNA targets (40). The ultimate verification of these RNA targets lies in the identification of gene transcripts that contain these sequences.

WT1 as a Transcription Factor

A number of WT1 target genes have been identified, including growth factors, growth factor receptors, and transcription factors, and it was found that WT1 could affect their promoter activity in transient transfection assays. It has been demonstrated, however, that the choice of cell system, the type of expression vector, or exact topology of the reporter construct can influence the transcriptional-regulating activity of WT1 proteins (1,41,42). For example, the WT1 (-KTS) isoform functions as a transcriptional repressor of the *EGR-1* promoter in NIH 3T3 cells (43), whereas it behaves as a transcriptional activator of the same promoter in both Saos-2 (44) and U2OS cells (45).

The specific roles for the different splice variants in the regulation of gene expression are unknown so far. Since both the +KTS and –KTS isoforms can bind DNA, however with different affinities, and it has been suggested that both splice variants may differentially regulate the same target genes. This is supported by the fact that both isoforms can bind overlapping DNA sequences in the promoters of the insulin-like growth factor 2 gene (46), the gene for platelet-derived growth factor-A (*PDGF-A*) (47), the *PAX-2* gene (48), and the *WT1* gene itself (49). The inclusion or exclusion of the 17 amino acid stretch from exon 5 does not seem to affect WT1's DNA binding ability, however, it does seem to exert an additional suppressor function in addition to the more N-terminal sequences (27,43,50). It has been found that the WT1 (+/+) protein, which includes sequences from both splice sites, suppresses the activity of the *WT1* promoter about 25 fold better than the WT1 (-/+) protein, which includes only the KTS motif, in transient transfection assays (49). It has also been observed that the WT1 (+/+) protein

represses transcription of the modified *PDGF-A* promoter construct whereas the WT1 (-/+) protein activates transcription (50). This suggests that the four splice variants may function as transcription factors with different regulatory abilities on target genes implicated in proliferation, differentiation, and cell cycle control.

WT1 as a Post-transcriptional Regulator

It is also possible that WT1 is involved in post-transcriptional processing of RNA. Nuclear staining of cells transfected with each of the four WT1 splice variants revealed that the +KTS isoforms preferentially localizes to subnuclear speckles and coiled bodies and colocalize predominantly with splicing factors (51). The –KTS isoforms exhibit a more diffuse pattern and are enriched in areas where the transcription factor, Sp1, is more abundant. Recently, the WT1 (+KTS) isoform has been shown to physically associate with small nuclear ribonucleoproteins (snRNPs) proteins of the splicing machinery, and this suggests that there is a role for the +KTS isoforms in splicing (51,52). More discussion on the interaction between WT1 and the splicing factors will follow in the section about WT1-binding proteins.

The major component of nuclear speckles and coiled bodies are splicing proteins (52). Coiled bodies were described originally as nucleolar accessory bodies and may play a role in the assembly, maturation, or recycling of the splicing complex. There is evidence that the nuclear speckles are dynamic structures and function perhaps as storage sites from which splicing factors are recruited. It has also been suggested that the subnuclear clusters may represent storage sites for WT1 isoforms with reduced DNA-

binding activity as WT1 mutants with disrupted DNA-binding domains also localize to the same clusters. It is possible then that at any given time, a significant proportion of WT1 may be stored in the speckles and not be actively involved in pre-mRNA processing. Nuclear speckles might reflect storage sites for both active and inactive or defective proteins involved in splicing. The functional proteins may be recruited subsequently to participate in pre-mRNA processing.

Significance of the WT1 (+KTS) and WT1 (–KTS) Isoforms

There is biochemical and genetic evidence to support the notion that the +KTS and –KTS isoforms are functionally different. The presence of both isoforms and the conservation of their ratios throughout the vertebrates (15) suggest that the insertion of the KTS is functionally important. The two isoforms have different but partially overlapping DNA binding affinities and specificities and this suggests that they regulate different sets of target genes (41). It may be that the primary role of the -KTS isoform is transcriptional regulation while the +KTS isoform is involved in other cellular processes (42). The subnuclear localization of the alternatively spliced isoforms suggests that they might have different functions at different sites in the nucleus. The –KTS isoform is localized diffusely throughout the nucleus whereas the +KTS isoform exhibits a speckled pattern within the nucleus (29,51). Genetic evidence for the distinct functional roles of the WT1 isoforms in urogenital development comes from WT1 mutations in the Fraiser syndrome, which results in a reduction in the +KTS: -KTS ratio (17,18,53).

Regulation of WT1

Activation of *WT1*

WT1 exhibits a very restricted temporal and spatial expression pattern. Currently, there is work towards the identification of cis and trans regulatory elements of WT1. PAX2 and PAX8, both members of the paired box family of transcription factors, and the zinc finger protein, SP1, all positively regulate the expression of *WT1* (54-56). *PAX2* is negatively regulated by WT1 (48). *PAX2* and *WT1* appear to be linked genetically, as *PAX2*-knockouts are similar in phenotype to *WT1*-knockouts; both lack kidneys and genital tracts (57). It is possible that both genes act in a common pathway. As well, WT1 negatively autoregulates its own promoter. This negative feedback loop could lead to the transient expression of *WT1* that is observed in various tissues (49,58).

Post-translational Modifications of WT1

The zinc fingers of WT1 are phosphorylated by Protein Kinase A (PKA) and Protein Kinase C in vitro (59), and exogenously expressed WT1 proteins in COS7 cells have been shown to be phosphorylated (60). Phosphorylation reduces the DNA binding activity of WT1 and the co-expression of PKA has been shown to reduce the ability of WT1 to repress transcription from two different promoters (59,60). Phosphorylation of endogenously expressed WT1, however, has not yet been verified. This is due to the low expression levels of the endogenous protein. N-terminal phosphorylation of WT1 has not been studied. As well, the upstream signals and kinases that regulate WT1 in the signal transduction cascade remain undefined.

Interacting Proteins of WT1

In cell lines that constitutively express WT1, most of the protein is found in protein complexes with molecular masses ranging from 100 to 669 kDa (44). It is possible that these high order protein complexes may involve WT1 multimers or WT1 associated with other cellular proteins (28,29,61). Modulation of WT1 activity by its interacting partner and vice versa can extend the functional capacity of both proteins **(Figure 2)**. Protein-protein interactions have been shown to alter the transcription regulatory functions of WT1 and implicate WT1 in the post-transcriptional event, splicing. Thus, identifying interacting proteins of WT1 may shed light on other roles for WT1 in the cell.

Proteins that Modulate WT1's Transcriptional Role

Prostate Apoptosis Response-4 Protein

The prostate apoptosis response 4 protein (PAR-4) was identified as an interacting partner of WT1 through yeast two-hybrid screens (62). The *PAR-4* gene was identified by differential screening for genes that are upregulated when prostate cancer cells are induced to undergo apoptosis (63). *PAR-4* expression is induced by apoptotic signals but not by growth-arresting, necrotic, or growth stimulatory signals. Unlike WT1, which exhibits tissue-restricted expression, *PAR-4* is expressed ubiquitously and is found in all the organs in which *WT1* is expressed (64). *PAR-4* is expressed in both the cytoplasm and nucleus, but expression levels are higher in the nucleus (62).

Figure 2:

WT1 interacting proteins. Yeast two-hybrid and immunoprecipitation experiments have identified a number of WT1-associated proteins. The first two WT1 zinc fingers stabilize another tumor suppressor gene product, p53. The zinc finger domain also interacts with two p53 homologues, p73 and p63. PAR-4, CIAO 1, and the human cytomegalovirus (HCMV) IE2 protein also bind the zinc finger region of WT1. The N-terminus of WT1 interacts with the human ubiquitin-conjugating enzyme 9 (hUBC9), the inducible chaperone Hsp70, and the steroidogenic factor 1 (SF-1). Splicing factor U2AF65 has been shown to bind the WT1 zinc finger region, however, the domain that interacts with some of the other splicing factors has not been characterized. The first 180 amino acids also harbor the dimerization domain of WT1.

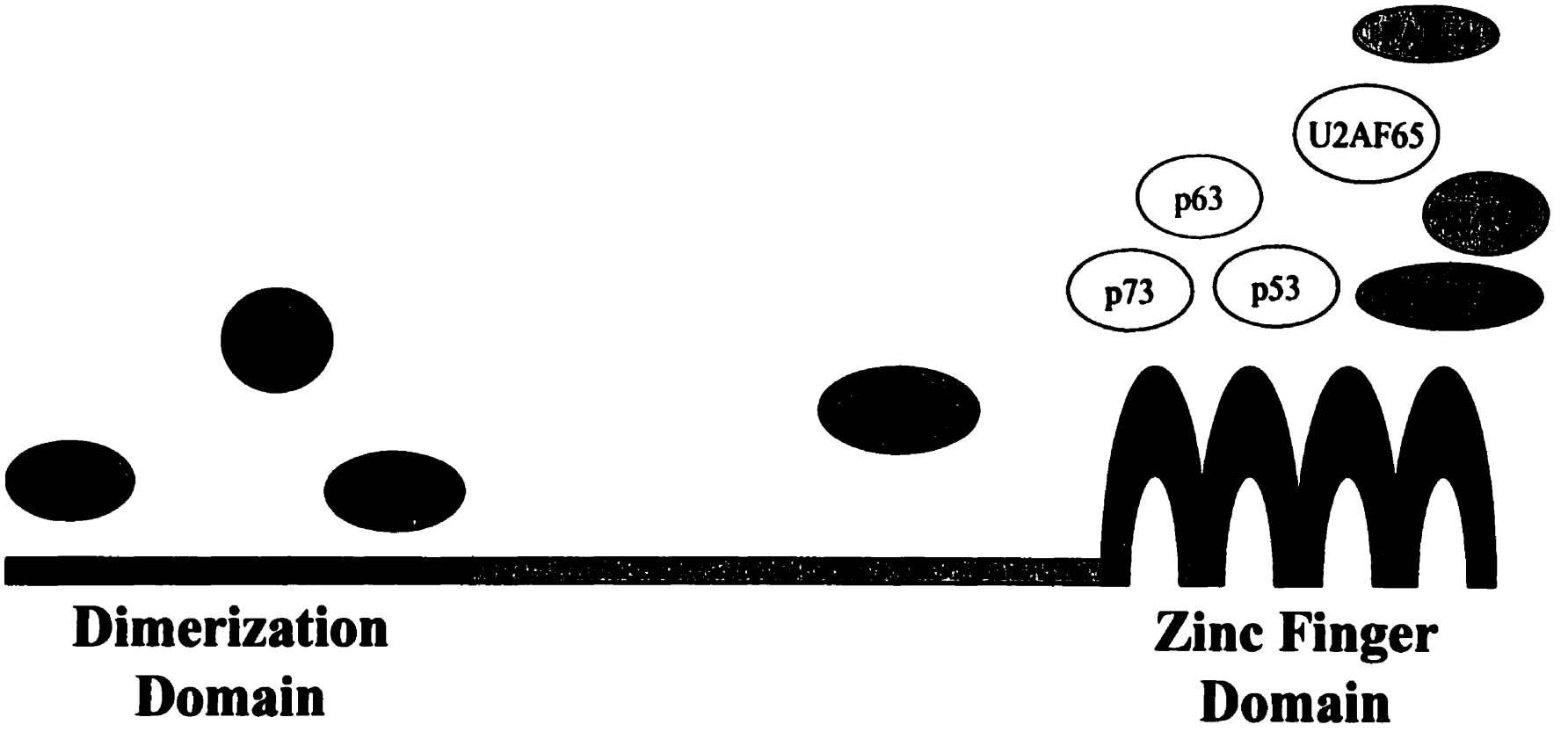
U2AF65
p63
p73
p53
Dimerization Domain
Zinc Finger Domain

PAR-4 interacts through its C-terminus leucine zipper domain with the zinc finger region of WT1 (62). The interaction between PAR-4 and WT1 appears to be specific and is not due to the general zinc finger structure as PAR-4 does not bind to the EGR-1 zinc fingers, nor does PAR-4 influence the transactivation function of the EGR-1 protein. PAR-4 interaction inhibits transcription activation by WT1 and enhances WT1-mediated transcription repression (62). Furthermore, overexpression of *PAR-4* can overcome the growth suppressive and anti-apoptotic effects of WT1 (65). This is consistent with the usual role of PAR-4 in activator-driven apoptosis. The requirement of PAR-4's leucine zipper domain for its effect on WT1 function illustrates the importance of PAR-4-WT1 binding for the regulation of apoptosis in co-transfected cells.

CIAO 1

CIAO 1 specifically interacts with WT1 both in vitro and in vivo (66). CIAO 1 is a member of the WD40 family of proteins containing β-transducin repeats (67,68). These proteins have a wide range of diverse biological functions including signal transduction, cell cycle regulation, RNA splicing, and transcription. The WD40 motif is thought to act as an interface for protein-protein interactions. *CIAO 1* is expressed ubiquitously and is detected in both cytoplasmic and nuclear cell fractions. The functional importance of *CIAO 1* is supported by the observation that its putative yeast homologue is an essential gene for viability. Therefore, CIAO 1 is believed to be an important cellular regulator whose functions may include the modulation of WT1-mediated transcription.

CIAO 1 binds the zinc finger domain of WT1 (66). CIAO 1-WT1 interaction has been shown to inhibit the transcriptional activation mediated by WT1. CIAO 1, however, does not affect the repression activity of WT1 and it does not inhibit WT1 binding to its consensus nucleotide sequence. CIAO 1 itself does not have any transcriptional repression activity. Its effect on the transcriptional activity of WT1 may be mediated through inducing conformational changes in the WT1 protein that would mask its activation function, or by negatively interfering with communication between the activation domain of WT1 and the basal transcriptional machinery.

p53, p73, and p63

p53 is the product of a tumor suppressor gene with ubiquitous expression. Physical association between WT1 and p53 modulates their respective transcriptional regulatory properties (44,69). In certain cellular settings and depending on the given reporter construct, p53 can convert WT1 from an activator to a repressor, whereas WT1 tends to exert a cooperative effect on transcription activated by p53 and reduce p53 repression. For example, in the absence of p53, WT1 acts as potent transcriptional activator of the *EGR-1* gene, rather than a transcriptional repressor, and WT1 has been shown to enhance p53's ability to transactivate muscle creatine kinase promoter. WT1 can also stabilize p53, requiring zinc fingers one and two to do so. WT1-binding inhibits p53-mediated apoptosis, without affecting p53-dependent growth arrest. There is plenty of evidence for WT1-p53 interaction in vivo but it is still not clear as to how this interaction leads to tumorigenesis given that *p53*-null mice do not show developmental abnormalities of the urogenital system (70).

Two-dimensional gel analysis shows that the WT1-p53 complex migrates at 100 to 150 kDa and contains individual components that migrate at approximately 50 kDa, allowing for either two or three such components within the complex (44). The association between WT1 and p53 could represent either direct binding or interaction through a third protein. From in vitro binding assays using purified proteins and in vitro translated proteins, it is believed that the interaction between WT1 and p53 is most likely direct (71). In adenovirus-transformed cells, WT1, which is normally localized in the nucleus, is retained in a high molecular weight complex with p53 and the adenoviral oncoprotein, E1B 55K, in a perinuclear cytoplasmic body (72). It is believed that WT1 binds to p53, which in turn interacts with E1B 55K to form the trimeric complex.

Two homologues of p53 have recently been cloned and both proteins are capable of binding WT1 in vitro and in vivo as well. The products of the *p73* (73) and *p63/p48/p51/KET* (74-77) genes share sequence homology with the transactivation, DNA binding, and tetramerization domains of *p53*. Both genes encode multiple isoforms as a result of alternative splicing. p73 and p63 can mediate transcription activation from p53-responsive elements and like p53, induce apoptosis (74,78). While *p53* is dispensable for embryonic development (79), *p73* and *p63* are intimately involved in differentiation and development (77,80,81). Their tumor suppressor functions have not yet been established.

p73 and p53 both bind to the zinc finger regions of all four alternative splice forms of WT1 (71). p73 binding inhibits DNA binding by WT1 possibly by shielding the zinc finger DNA binding domain of WT1, an effect not observed with p53. Consequently, p73 represses WT1-mediated transcription activation. WT1 is also capable of repressing p73 and p53-induced transcription activation of the endogenous

MDM2 gene, however, the effects of WT1, measured in transient reporter assays with equal amounts of p73 and p53 expression constructs, appear to be stronger on p73 than on p53.

WT1 may be involved in two different cellular pathways with regard to the p53 family members: p53-regulated cell proliferation and p73 and p63-mediated developmental regulation. Reduction of MDM2 protein levels through a WT1 effect on p53 and p73 transcription activation may slow down MDM2-triggered degradation of p53 and thus lead to higher p53 protein levels (71). At the same time, binding of WT1 to p53 may inhibit MDM2 from targeting p53 for degradation. MDM2 binds to p73 without targeting it for degradation and therefore is not stabilized by WT1. As well, WT1 is capable of inhibiting degradation of p53 by the human papiloma virus E6 protein, which interacts with p53, but not with p73 (69). There is also evidence to suggest that WT1 may modulate p53 function in response to stress (69,82). It is possible then that WT1, a tissue-specific and developmentally-regulated transcription factor, may be involved in regulating fundamental processes associated with differentiation and development with p73 and p63 while regulating cell growth in concert with p53.

Human Cytomegalovirus IE2 Protein

The IE2 protein of the Human Cytomegalovirus (HCMV) interacts with the zinc finger domain of WT1 in vivo and in vitro (83). HCMV is the major renal pathogen in congenitally infected infants and renal allograft recipients (84,85). The *IE2* gene is expressed in the immediate early stage of the viral life cycle and regulates viral gene expression between the immediate-early and later stages (86). IE2 is a potent transactivator of many cellular and viral promoters. It binds to cellular transcription

factors, for example, TBP and TFIIB (87,88), and also to tumor suppressor proteins, such as, p53 (89) and Rb (90). HCMV IE2 protein also interacts directly with the zinc finger domain of EGR-1 (91).

WT1 binding to IE2 inhibits IE2-mediated transcriptional activation of a *PDGF-A* reporter construct (83). It is speculated that this negative regulation occurs in a similar fashion to the Rb-IE2 interaction. Since IE2 is required for the expression of the HCMV genes involved in the later stages of the viral life cycle, the tumor suppressor proteins, WT1 or Rb, would effectively provide a means by which the host cell can delay the replication of the virus by binding to and inhibiting the transactivation activity of IE2 (90). Conversely, this interaction may also result in the functional inactivation of the tumor suppressor gene product as in the adenoviral protein E1B 55K sequestration of WT1 and p53 within the cytoplasmic bodies of adenovirus-transformed kidney cells (72).

Proteins that Implicate WT1 in the Post-transcriptional Event, Splicing

In addition to evidence showing that WT1 is capable of binding RNA in vitro and colocalization data showing association of WT1 (+KTS) isoforms with splicing factors, the identification of WT1 binding partners that are splicing factors provides further support that WT1 is involved in post-transcriptional events. Larson et al. (51) found that WT1, mostly the +KTS isoform, co-immunoprecipitates with snRNPs, splicing factors U170, U2B", and p80 coilin. Davies et al. (52) described the interaction between WT1 and the ubiquitous splicing factor U2AF65. They also found that WT1 and the splicing factor U2-B" assembled in vitro into large molecular weight complexes that are

associated with the sense but not the antisense strand of a biotinylated adenoviral pre-mRNA.

There is also evidence to suggest that WT1 is present in nuclear poly (A)+RNP (92). Oligo(dT) chromatography shows an enrichment of WT1 and various splicing factors including U2AF65, the U5 small nuclear RNP-associated protein p116, and human ribonucleoprotein (hnRNP) A1. Gel filtration and sedimentation profiles suggest that WT1 is present in RNAse-sensitive particles of greater than 2 MDa in size, peaking at approximately 60 S. While it is unlikely that WT1 is a component of the core hnRNP particle, WT1 does sediment in a single spliceosome range of between 40 and 60 S along with p116. There seems to be a preference for co-sedimentation of WT1 with p116 as opposed to U2AF65 or hnRNP A1 and this interaction is further supported by double labeling experiments in cultured cells indicating a significant degree of colocalization of WT1 (+KTS) isoform with p116. These results should be interpreted with caution as they do not attest to a direct interaction between WT1 and p116 nor that WT1 is in fact involved in splicing.

In light of the data obtained from the co-sedimentation experiments, it is possible that only a small fraction of WT1 interacts with U2AF65 at any given time. Recent work suggests that a large fraction of U2AF65 appears not to be associated with spliceosomes (93) or that in vitro buffer conditions do not provide optimal conditions for interaction. This issue still needs to be resolved.

It is the C-terminus, but not the N-terminus, of WT1 that is responsible for the enrichment of WT1 into poly(A)+ fractions (92). This suggests that a predicted RNA recognition motif at the N-terminus of WT1 (94) is not required for nuclear localization

and incorporation into the RNP. WT1 isoforms containing or lacking the first alternative splice exon and isoforms due to the alternative upstream translation start sites are all present within the RNP particles.

U2AF65

Davies et al. (52) showed that the WT1 (+KTS) isoform colocalizes and associates with splicing factor U2AF65(52). During splicing, U2AF65 targets the 3' splice acceptor site and binds to its partner, U2AF35, to promote the annealing of U2snRNA to the polypyrimidine tract adjacent to the 3' splice site, facilitating splicing (95). Splicing proteins display a nuclear speckled pattern and have several common motifs, including arginine/serine-rich RS domains and RNA recognition motifs (RRM). Evidence from molecular modeling suggests that WT1 may have an N-terminus RRM (94). RNA binding by WT1 has been demonstrated in vitro and mapped to the first zinc finger of WT1, which has a slightly different structure than the other three zinc fingers (39). WT1 binds to the RS domain of U2AF65 (52), which is slightly different from the classical RS domains (96). WT1 does not interact with other RS proteins, such as U2AF35. U2AF65 RS domains promote the RNA-RNA interaction between U2snRNA and the branch point (96) and it is possible that it is this function of UAF65 that WT1 affects. Through interaction with U2AF65, it is possible that WT1 can be incorporated directly into the spliceosome complex and that WT1 could therefore influence the 3' splice site selection in a cell-type or temporal-dependent manner. WT1 would then select a particular 3'splice site and present this directly to the RRM of U2AF65.

U2AF65 binds the zinc finger region of WT1 (52). It is possible that the + and - KTS isoforms adopt different conformations that render the -KTS isoform with stronger

DNA-binding ability and weaker U2AF65-binding ability, and conversely for the +KTS isoform. It is interesting then to consider that mutations commonly found in Denys-Drash syndrome patients affecting the zinc finger residues result in an apparent increase in U2AF65 binding by the -KTS isoform with a decrease in DNA binding. Fraiser syndrome, on the other hand, has mutations at the splice donor sites that specifically perturb the isoform ratio and favors an excess of the –KTS isoform (17). Davies et al. (52) suggested that by WT1 dimerization, one molecule of WT1 with strong DNA-binding ability could be coupled to another with high U2AF65 affinity. Through such cooperation between the +KTS and -KTS isoforms, the correct amount of transcript synthesized and correctly spliced can be monitored.

Other Interacting Proteins of WT1

Human Ubiquitin-Conjugating Enzyme 9

The human ubiquitin-conjugating enzyme 9 (hUBC9) was identified by a yeast two-hybrid screen to interact with the proximal negative regulatory domain, amino acids 85 to 179, of the WT1 protein (97). While it is unclear at this point how these two proteins affect each other's activities, it is speculated that hUBC9 could modulate WT1's repression activity.

The hUBC9 gene encodes a 17 kDa protein that has 56% amino acid sequence homology with the yeast ubiquitin-conjugating enzyme 9 (yUBC9), a protein required for cell cycle progression in yeast, and having significant homology to other subfamilies of ubiquitin-conjugating enzymes (97). The ubiquitin-dependent protein degradation system is responsible for the selective degradation of many abnormal and short-lived

proteins (98,99). Ubiquitin is covalently linked to target proteins prior to their degradation through the combined action of three classes of proteins: the ubiquitin activating enzyme (E1), the ubiquitin-conjugating enzymes (E2), and in some cases, the ubiquitin-protein ligases (E3), that are believed to be important in substrate recognition. The diversity and the multiple protein-protein interactions of the ubiquitin-dependent proteolytic system suggest that a high degree of regulation is required to achieve the specificity needed to control the fate of the different proteins that are degraded through ubiquitination. While it is very likely that the E2 enzymes may contribute to the determination of which groups of proteins are targeted for selective degradation, WT1 interaction with hUBC9 may very well influence this selection.

WT1-hUBC9 interaction may also play an important role in the regulation of the cell cycle. The yUBC9 is involved in cell cycle progression. It is required for the degradation of S- and M- phase cyclins and for cell viability (100). Since the hUBC9 can fully complement yUBC9 temperature-sensitive mutants to allow normal progression of yeast cells through the cell cycle, it is possible that hUBC9 plays a similar role in eukaryotic cells. WT1 is capable of blocking cell cycle progression and this block can be relieved by the expression of exogenous cyclin E and CDK2 as well as cyclin D1/CDK4 (100). In light of hUBC9's role in the cell cycle, the WT1-hUBC9 interaction is probably important to the cell cycle block mediated by WT1.

Heat Shock Protein 70

Heat shock protein 70 (Hsp70) was identified as a binding partner of WT1 through co-immunoprecipitation experiments (101). Physical association between Hsp70

and WT1 has been observed in embryonic rat kidney cells, primary Wilms' tumor specimens, and cultured cells with inducible expression of WT1. Colocalization of WT1 and Hsp70 is evident within the glomerular podocytes of the developing kidney, where Hsp70 is recruited to characteristic subnuclear compartments that contain WT1.

The extreme N-terminal domain of WT1, amino acids 6 to 180, is required for interaction with Hsp70 (101). The expression of the N-terminal domain itself is sufficient to induce expression of *Hsp70* through an unidentified mechanism thought to involve the regulatory heat shock element of the *Hsp70* promoter - transcriptional activation of the *Hsp70* promoter by the WT1 N-terminus occurs independent of WT1's DNA binding activity. Induction of *Hsp70* by WT1 and physical association between the two proteins suggest that Hsp70 plays an important role in the cellular differentiation pathway. This is consistent with its apparent contribution to the steroid hormone response pathways and hematopoietic differentiation (102,103). Hsp70 binding is required for WT1 to function as an inhibitor of cellular proliferation, which correlates with WT1's known function as a tumor suppressor gene (101). This suggests that Hsp70 is an important cofactor for the proper functioning of WT1 and that a potential role for Hsp70 is as a chaperone during kidney differentiation.

Heat shock proteins are a highly conserved family of molecular chaperones with diverse functions, including mediating protein folding and degradation, transport across cellular membranes, and assembly into macromolecular structures (104,105). The inducible Hsp70 proteins are expressed at low levels physiologically but are rapidly induced following growth of cells at 40°C (106). During growth at the physiological temperature, *Hsp70* expression is tightly regulated during cell cycle progression (107)

and it is induced by stimuli that induce cellular proliferation, including serum (108), expression of c-myc (109), viral oncoproteins adenovirus E1A (110), and large T antigen from SV40 and polyoma viruses (111).

Similar amounts, approximately 25%, of cellular Hsp70 and WT1 associate with each other in rat kidney cells, indicating that a significant fraction of these cellular proteins are associated with each other in the cell (101). A parallel pattern of expression for both WT1 and Hsp70 is also observed in the embryonic kidney, both in terms of specific cell type and subcellular localization. There is a speckled nuclear expression pattern for both in the glomerular podocytes and expression of both proteins is reduced in the adult kidney. This suggests that the interaction between WT1 and Hsp70 is developmentally regulated. Since heat shock protein family members are well-known for binding denatured or misfolded proteins, it is possible that the physical association between WT1 and Hsp70 is for the purpose of ensuring the correct molecular folding of the rigid proline-rich N-terminus of WT1. This may then serve to enhance the functional properties of WT1 and potential interactions with other proteins.

Steroidogenic Factor-1

WT1 is a transcriptional coactivator of the orphan nuclear hormone receptor Steroidogenic Factor-1 (SF-1) during mammalian gonadogenesis (112). Physical association between the N-terminus of WT1 and SF-1 dramatically increases the transactivational activity of SF-1. Functional synergy occurs only with the WT1 (–KTS) isoform.

SF-1 is an important regulator of male sexual development after testis determination. SF-1 exhibits high affinity DNA-binding and is a positive transcriptional regulator of a variety of steroidogenic enzyme genes in adrenal glands and gonads, including male-specific genes (113,114). In mice that lack *SF-1*, the gonads and adrenal glands fail to develop, and these mice have hypogonadotropic hypogonadism, indicating hormone deficiencies at the hypothalamic and pituitary gland levels (115). Similarly, *WT1*-null mice of both sexes fail to develop kidneys and gonads, indicating that WT1 acts upstream of sex-determination (11).

A close functional relationship exists between SF-1, DAX-1, and WT1 proteins (112). Dosage-sensitive Sex-reversal Adrenal Hypoplasia Congenita Critical Region on the X chromosome, gene 1 (DAX-1) is also an orphan nuclear hormone receptor that plays a critical role in the development of adrenal gland and reproductive systems (116). As with *SF-1*, transcripts of the *Dax-1* gene can be detected in specific endocrine tissues: the hypothalamus, anterior pituitary, adrenal glands, gonads, and placenta. During mouse urogenital development, the expression profiles of both SF-1 and DAX-1 are sexually dimorphic (117) and interference by DAX-1 of the SF-1/WT1 interaction will lead ultimately to ovarian development by modulating SF-1-mediated transactivation. While physical association between WT1 (–KTS) and SF-1 is observed in the yeast two hybrid system, as with DAX-1 and SF-1 (112), no interaction was observed between DAX-1 and WT1. The major sites of interaction on SF-1 for DAX-1 and WT1 appear to be distinct. WT1, therefore, most likely has a male-specific function in the sex determination pathway.

Objective

We are interested in other endogenous cellular proteins that interact with WT1, in particular, nuclear proteins that target the WT1 (–KTS) zinc finger domain. We aimed to utilize affinity chromatography to identify putative nuclear proteins that interact with WT1.

METHODS AND MATERIALS

Cell Culture and Preparation of HeLa Cell Nuclear Extracts

Fifty (150 mm) plates of HeLa S3 cells were grown to confluency for the preparation of nuclear extracts. Cells were maintained in DMEM with 10% fetal calf serum, penicillin (100 U/ml) and streptomycin (100 µg/ml), and L-glutamine (4 mM) (Gibco BRL), and grown at 37°C in a humidified 5% CO_2 incubator. The cells were harvested by scraping in cold phosphate buffered saline (PBS) and pelleted by centrifugation for 5 minutes at 1500 rpm and 4°C. The cells were washed by resuspending in PBS and centrifuging again. The pellet was resuspended in 5 ml of Buffer A [10 mM $Hepes_{7.9}$; 1.5 mM $MgCl_2$; 10 mM KCl; 0.5 mM DTT] with protease inhibitors benzamidine-HCl, PMSF, leupeptin, and antipain (1 mM of each). The cells were lysed mechanically using a type B dounce and lysis was verified by staining the cells with trypan blue. The lysate was then centrifuged at 4°C for 15 minutes at 1500 g's to pellet the nuclei. The supernatant was removed and the pellet, consisting largely of nuclear components, was resuspended in 5.5 ml of 75 mM NaCl Affinity Chromatography (AC) Buffer [20 mM $Hepes_{7.5}$; 10% glycerol; 1 mM DTT; 1 mM EDTA] with protease inhibitors and sonicated for 60 seconds (2 bursts of 30 seconds) at 4°C. The lysate was then centrifuged at 4°C for 30 minutes at 20,800 g's.

Purification of GST and GST-WT1 Zinc Finger Proteins

pGEX-RC and pGEX-RC WT1 Zinc Finger (ZF) plasmids, that have been previously described (118), were transformed into BL21 bacteria (119). Two liter cultures of the

bacteria were grown in LB media containing 100 μg/ml ampicillin at 37°C with shaking until OD_{600}= 0.9, at which point the cultures were induced for 3 hours at 37°C with 1 mM (final concentration) IPTG. The cultures were then centrifuged at 4°C for 20 minutes at 3000 g's. The bacterial pellet was resuspended in 50 ml of Extraction Buffer [1x PBS; 0.1 mM EDTA; 2mM DTT] with protease inhibitors and sonicated for 2 minutes (4 bursts of 30 seconds). The lysate was then centrifuged at 4°C for 30 minutes at 12,100 g's to pellet the cellular debris. The lysate obtained was then applied to 1 ml (bed volume) of glutathione sepharose 4B (Pharmacia Amersham Biotech) that had been pre-washed 3 times with the Extraction Buffer. Washing was performed by resuspending the beads with the buffer and then centrifuging at 4°C for 5 minutes at 1500 g's. The beads and the lysate were incubated end over end at 4°C for 1 hour to allow binding to occur. The beads and the lysate were then centrifuged at 4°C for 5 minutes at 1500 g's and and the lysate was removed. The beads were then washed with 10 ml of the Wash Buffer [1x PBS; 0.1 mM EDTA; 2 mM DTT; 1% Triton X-100) 3 times with repeated resuspension and centrifugation. Elution was carried out with ten 1 ml volumes of Elution Buffer [10 mM glutathione in AC Buffer] whereby the beads were incubated with 1 ml of the Elution Buffer with periodic mixing for 5 minutes and centrifuged briefly. Aliquots of each fraction were fractionated by SDS-PAGE on 12.5% polyacrylamide gels and the proteins were visualized by coomassie staining. The concentrations of the proteins were determined by the Bradford Assay.

Affinity Chromatography

One hundred microliters (bed volume) of Affigel 10 resin (BioRad) were used per sample. The resin was washed 3 times with cold ddH_2O (by repeated resuspension and centrifugation). GST WT1 ZF protein was coupled to the Affigel 10 resin at protein/resin concentrations of 0, 0.5, or 2.0 mg/ml in a final volume of 200 µl of AC Buffer. As a control, GST protein was coupled to the resin at protein/resin concentrations of 0 or 2.0 mg/ml. Coupling was performed by incubating overnight at 4°C with continuous end over end movement. The supernatant was saved for later determination of the coupling efficiency by Bradford Assay. The resin/protein was incubated sequentially with 75 mM NaCl AC Buffer with 80 mM ethanolamine for 1 hour followed by 75 mM NaCl AC Buffer containing 1 mg/ml purified bovine serum albumin (BSA) for 30 minutes, both at 4°C. The matrix was then washed with 1 M NaCl AC Buffer for 10 minutes and then equilibrated with 75 mM NaCl AC Buffer by washing 3 times. Ten column volumes (1 ml) of the HeLa cell nuclear extract was applied to the matrix for 1 hour with end over end incubation. As control, 1 ml of 75 mM NaCl AC Buffer was applied to a similar matrix. In addition, HeLa extracts were also loaded onto GST-immobilized columns. The resin was then washed three times with 75 mM NaCl AC Buffer. Elution was performed sequentially with 2 times 2 column volumes (2 times 200 µl) of each of the following: 75 mM NaCl AC Buffer with 1% Triton X-100; 300 mM NaCl AC Buffer; 1 M NaCl AC Buffer; and 1% SDS AC Buffer. Forty microliters of each fraction were analyzed by SDS-PAGE on 12.5% polyacrylamide gels and proteins were visualized by silver staining.

Silver Staining

Gels were prepared for silver staining by fixing overnight in 50% methanol/10% acetic acid, and then rinsing for 10 minutes in 20% ethanol and 10 minutes in water. Gels were then reduced with sodium thiosulfate (0.2 g/l) for 1 minute and then rinsed twice with water for 20 seconds each wash. Gels were then incubated in silver nitrate (2.0 g/l) for 30 minutes. Gels were washed once with developing solution [sodium carbonate 30 g/l; formaldehyde 1.4 ml of 37% solution/l; sodium thiosulfate 10 mg/l] for 30 seconds, and then incubated in the developing solution until the desired intensity was reached. The reaction was stopped by exchanging the developing solution with 1% acetic acid for a minimum of 20 minutes. Bands of interest were excised with clean scalpels and twenty microliters of 1% acetic acid were added to the gel slices which were quick-frozen on dry ice and stored at –70°C.

Protein Identification by Mass Spectrometry

Gel slices containing a single 32 kDa band were sent to Borealis Biosciences Inc. (Toronto, Canada) for identification by MALDI-ToF Mass Spectrometry. The gel slices containing the candidate protein were processed and digested overnight with the protease, trypsin, to produce proteolytic peptides that were then prepared for mass spectrometry with a PerCeptives Biosystems Voyager Elite MALDI-ToF. Identification of the candidate protein by mass spectrometry was made according to the masses of its proteolytic peptides. The protein was identified by matching the observed proteolytic

masses in the MALDI-ToF spectra with the hypothetical proteolytic peptide masses derived from non-redundant translated genomic databases.

Cloning of BMZF2 by RT-PCR

The BMZF2 cDNA was obtained from a reverse transcriptase (RT) reaction from HeLa cell mRNA. The reaction mixture consisted of 2 μg of HeLa cell mRNA; 0.15 μg of N_6 random primers (Pharmacia Amersham Biotech); and 10 U/μl of SuperScript II (LTI), utilized with conditions recommended by the manufacturer. The reaction mixture was incubated at 25°C for 10 minutes, 42°C for 1 hour, and 70°C for 15 minutes. The reaction mixture was then diluted to a final volume of 200 μl. Polymerase chain reaction (PCR) amplification was performed on the diluted first strand reaction using the Peltier Thermal Cycler PTC-200 (MJ Research). The PCR mixture consisted of 2 μl of the diluted 1st strand reaction; 0.2 μM of each of the forward and reverse primers; 0.4 mM dNTPs; 2 mM $MgSO_4$; 1x Hi-Fi Buffer; and 0.5 U of Platinum Taq DNA Polymerase High Fidelity (LTI) in a total volume of 25 μL. The forward and reverse primers were BMZF2 5' Xho I [5'GATCCTCGAGATGGAGACTGTTTCAGAA3'] and BMZF2 3' Hind III [5'GATCAAGCTTCTAAGGTTTTTCTCCAAC3'] which target the start and stop codons of the *BMZF2* gene. Cycling parameters for the Touchdown PCR reaction were 94°C for 5 minutes; 94°C for 1 minute, 65°C for 1 minute, and 68°C for 2 minutes – all for 5 cycles with a negative ramp of 2 °C/cycle; 94°C for 1 minute, 55°C for 1 minute, and 68°C for 2 minutes – all for 30 cycles; and 68°C for 10 minutes. The RT-PCR product was analyzed by gel electrophoresis on a 1% agarose gel with 2 μg/ml of

ethidium bromide and visualized under UV light. The RT-PCR product was then digested with the restriction enzymes Xho I and Hind III, corresponding to the sites incorporated into the primers, and ligated into the vector, pBluescript KSII+ (pksII+), which was digested with the same enzymes. Several clones were sequenced using the T7 Polymerase Sequencing Kit (Pharmacia Amersham Biotech) to verify that the sequence was correct.

Direct Sequencing

During sequencing of the BMZF2 gene, we noticed several differences between our clones and the one deposited in public databases (GenBank Accession #: AF067164). To resolve these, direct sequencing was performed directly on product derived from an RT-PCR reaction. An RT-PCR reaction was performed as described above on 2 μg of human fetal brain mRNA (CLONTECH) and analyzed on a 1% agarose gel. PCR primers were BMZF2 5' Xho I and N-terminus Reverse 3' EcoR I [5'CCCGGAATTCAAAATCAAAGAGGGAGACATCACTGAA3'] primer, which targets nucleotides 217 to 243 of the BMZF2 gene ORF. The RT-PCR product was excised from the gel and purified using the Qiaex II Gel Extraction Kit (Qiagen) into a 30 μL volume. Direct Sequencing was performed with the aid of the *fmol* DNA Sequencing System (Promega) on 4 μl of the purified template. Some reagents were not supplied by the kit, such as, T4 Polynucleotide Kinase (NEB) and ATP (γ-^{33}P) (NEN). Sequencing products were electrophoresed on a 6% denaturing polyacrylamide gel. The gel was dried and exposed to Kodak X-Omat film overnight.

In Vitro Transcription and In Vitro Translation

Plasmid KSII-BMZF2 plasmid was linearized with the Sma I restriction enzyme and used as a template for in vitro transcription. The reaction mixture, in a total volume of 100 µl, consisted of 1 µg of linearized DNA; 10 mM DTT; 0.5 mM of each ATP, GTP, CTP, UTP; 0.5 mM of the RNA Cap Structure Analog $m^7G(5')ppp(5')G$ (NEB); 80 U of RNAguard RNase Inhibitor; 1x RNA Polymerase Buffer; and 200 U of T7 RNA Polymerase (NEB) added to 10 µl of cytidine 5'-triphosphate tetrasodium salt [5-^{3}H] (NEN) which had already been lyophilized in a 1.5 ml eppendorf tube. The reaction mixture was incubated at 37°C for 2 hours. The in vitro transcription product was purified by phenol/chloroform extraction, G-50 sephadex spun column, and ethanol precipitation. The RNA pellet was washed with 70% ethanol, dried, and resuspended in 30 µl of water. In vitro translation was performed with the aid of the Rabbit Reticulocyte Lysate System (Promega) on approximately 1 µg of BMZF2 mRNA in the presence of EASYTAG L-[^{35}S]-methionine (NEN) and RNAguard RNase Inhibitor. The reaction mixture was incubated at 30°C for 60 minutes. Five microliters of the in vitro translation product were analyzed by SDS-PAGE on 12.5% polyacrylamide gels. Gels were then fixed in 40% methanol/10% acetic acid, treated with En^{3}Hance Autoradiography Enhancer (NEN) for 30 minutes, washed with water for 20 minutes, dried, and exposed to Kodak X-Omat film at –70°C overnight. In vitro transcription and in vitro translation were performed similarly on a plasmid containing the human p53 cDNA obtained from the lab of Dr. John White (McGill University).

GST Pulldown Assay

Twenty microliters (bed volume) of glutathione sepharose 4B resin were washed 3 times with 200 µl (10 bed volumes) of GST Buffer [50 mM Tris-$Cl_{7.5}$; 100 mM NaCl; 10 mM $MgCl_2$; 10% glycerol; 1% Triton X-100; 0.3 mM DTT]. Five micrograms of GST or GST WT1 ZF proteins were bound to glutathione resin in a total volume of 200 µl of GST Buffer by incubating 1 hour at 4°C with continuous end over end movement. The resin was then pelleted and washed twice with 200 µL of GST Buffer. Five microliters of the in vitro translated protein, BMZF2 or p53, were then applied to the GST or GST WT1 ZF/resin in a total volume of 200 µl of GST Buffer. Binding was performed by incubating 1 hour at 4°C with continuous end over end movement. The resin was then pelleted and the flowthrough was collected and saved for analysis later. The resin was washed 3 times with GST Buffer and eluted with 80 µl of SDS Sample Buffer. Forty microliters (50%) of the elution and 40 µl (20%) of the flowthrough were loaded onto 12.5% polyacrylamide gels and analyzed by SDS-PAGE. The gels were coomassie stained, treated with En^{3}Hance, dried, and exposed to Kodak X-Omat film at –70°C overnight.

RESULTS

Isolation and Identification of a New Potential WT1-Interacting Protein

The WT1 protein has been reported to bind a number of proteins, including PAR-4, CIAO 1, and p53 (44,62,66). We utilized affinity chromatography and immobilized the zinc finger domain to determine which, if any, WT1 interacting partners could be isolated from nuclear extracts prepared for HeLa cells. To this end, HeLa cell nuclear extracts were incubated with Affigel 10 resin which had been coupled to GST or GST WT1 ZF fusion proteins, as described in the Materials and Methods. The affigel/GST resin served as a control for non-specific interactions. Proteins bound to the affinity resins were washed with a series of buffers differing in salt and detergent concentrations.

Silver stained SDS-PAGE gel 1 shows the input as 40 µl, out of 1 ml, of the HeLa cell nuclear extract that was applied to the GST or GST WT1 ZF-coupled resin (**Figure 3a, Lane 1**). The subsequent lanes show 40 µl, out of 1 ml, of the flowthrough collected after binding (**Figure 3a, Lanes 2 to 8**). Forty microliters (20%) of each elution is shown in each lane of gels 2, 3, 4, 5, and 6 (**Figures 3b, c, d, e, and f**). One percent Triton X-100 AC Buffer eluted predominantly proteins that bound non-specifically to the matrix, as bands that appear in the GST WT1 ZF lanes (**Figure 3b, lanes 5, 6, and 7**) are also present in the GST lanes (**Figures 3b, lanes 2 and 3**), at all concentrations of protein/resin coupled. Multiple bands were eluted specifically from the GST WT1 ZF matrix and not from the GST matrix at both the 300 mM NaCl AC Buffer and the 1 M NaCl AC Buffer elutions (**Figure 3c and d, lanes 6 and 7 *indicated with arrows***). Those bands that appeared in 0.5 mg/mL GST WT1 ZF protein/resin lanes also appeared in the 2.0 mg/ml protein/resin lanes and with higher intensity. Furthermore, fraction 2 of

Figure 3:

Isolation of a new potential WT1-interacting protein. HeLa cell nuclear extracts were incubated with Affigel 10 resin coupled to GST or GST WT1 ZF. **(a)** The input lane represents 40 µl, out of 1 ml, of the HeLa cell nuclear extract that was applied to the GST or GST WT1 ZF-coupled resin (lane 1). The subsequent lanes represent 40 µl, out of 1 ml, of the flowthrough that was collected after binding (lanes 2 to 8). After a series of washes, the resins were eluted sequentially with buffers of increasing stringency: **(b)** 1% Triton X-100 Affinity Chromatography (AC) Buffer; **(c)** 300 mM NaCl AC Buffer; **(d)** 1 M NaCl AC Buffer; **(e)** 1% SDS AC Buffer; and **(f)** SDS Sample Buffer. Forty microliters (20%) from each elution were then analyzed by SDS-PAGE on 12.5% polyacrylamide gels and silver-stained. Proteins of approximately 62 kDa prevailed across all the lanes and probably corresponded to BSA, which had been used in pre-blocking. **(b)** One percent Triton X-100 AC Buffer eluted predominantly proteins that bound non-specifically to the matrix, as bands that appear in the GST WT1 ZF lanes (lanes 5, 6, and 7) are also present in the GST lanes (lanes 2 and 3), at all concentrations of protein/resin coupled. **(c)** Multiple bands were eluted specifically from the GST WT1 ZF matrix and not from the GST matrix at the 300 mM NaCl AC Buffer (lanes 6 and 7, indicated with arrows). Those bands that appeared in the 0.5 mg/mL GST WT1 ZF protein/resin lanes and in the 2.0 mg/ml protein/resin lane. **(d)** The 1 M NaCl AC Buffer elution yielded a singular protein of approximately 32 kDa in size (lanes 6 and 7, indicated by arrow). **(e and f)** Elutions with 1% SDS AC Buffer and SDS Sample Buffer also revealed proteins that bound non-specifically to the matrix as well as coupled proteins that had leached off the resin. Bands that appeared in the GST WT1 ZF and nuclear extract lanes (lanes 6 and 7) are also present in the lanes where no GST or GST WT1 ZF fusion had been coupled (lanes 2 and 5) and the lanes where GST or GST WT1 ZF fusion had been coupled but no extracts were applied (lanes 1 and 4).

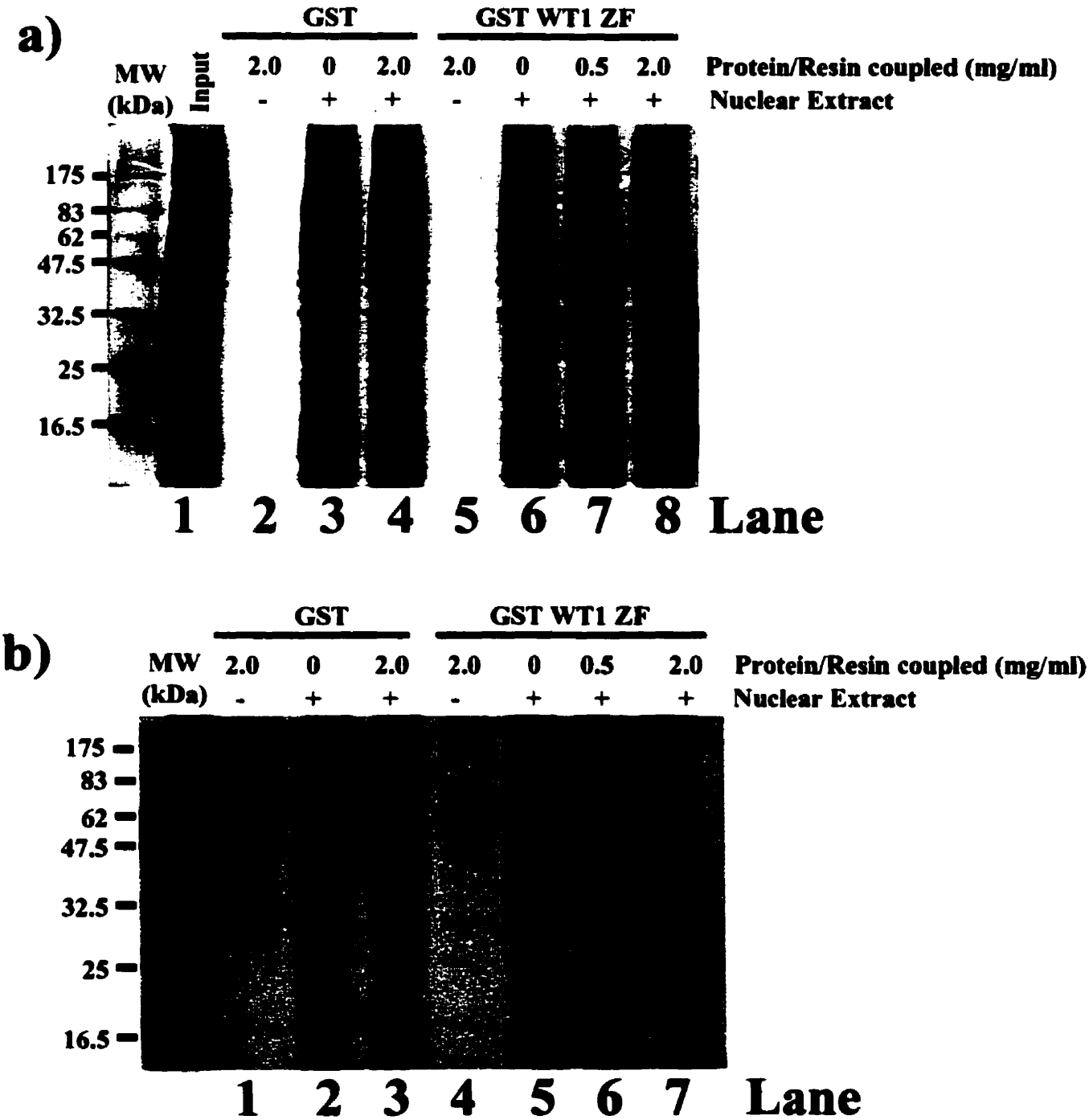
a)
GST
GST WT1 ZF
MW (kDa)
Input
2.0 0 2.0 2.0 0 0.5 2.0
Protein/Resin coupled (mg/ml)
- + + - + + +
Nuclear Extract
175
83
62
47.5
32.5
25
16.5
1 2 3 4 5 6 7 8 Lane
b)
GST
GST WT1 ZF
MW (kDa)
2.0 0 2.0 2.0 0 0.5 2.0
Protein/Resin coupled (mg/ml)
- + + - + + +
Nuclear Extract
175
83
62
47.5
32.5
25
16.5
1 2 3 4 5 6 7 Lane

c)

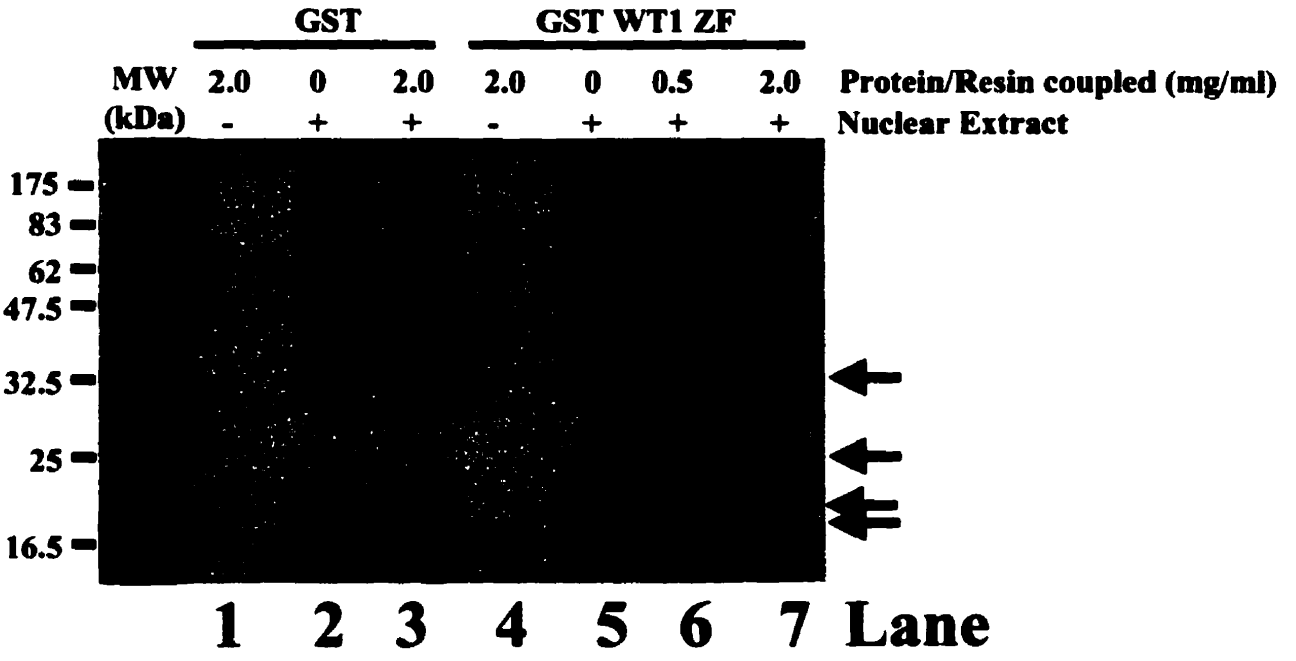
GST
GST WT1 ZF
MW
(kDa)
2.0 0 2.0 2.0 0 0.5 2.0
- + + - + + +
Protein/Resin coupled (mg/ml)
Nuclear Extract
175
83
62
47.5
32.5
25
16.5
1 2 3 4 5 6 7 Lane

d)

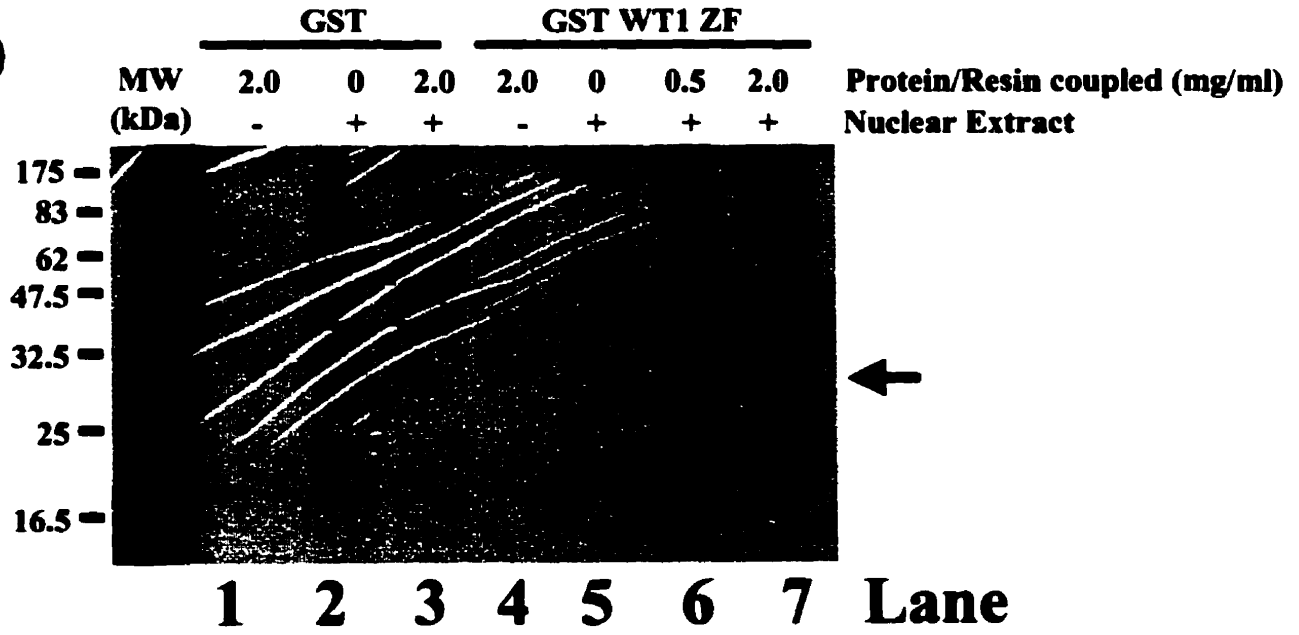
GST
GST WT1 ZF
MW
(kDa)
2.0 0 2.0 2.0 0 0.5 2.0
- + + - + + +
Protein/Resin coupled (mg/ml)
Nuclear Extract
175
83
62
47.5
32.5
25
16.5
1 2 3 4 5 6 7 Lane

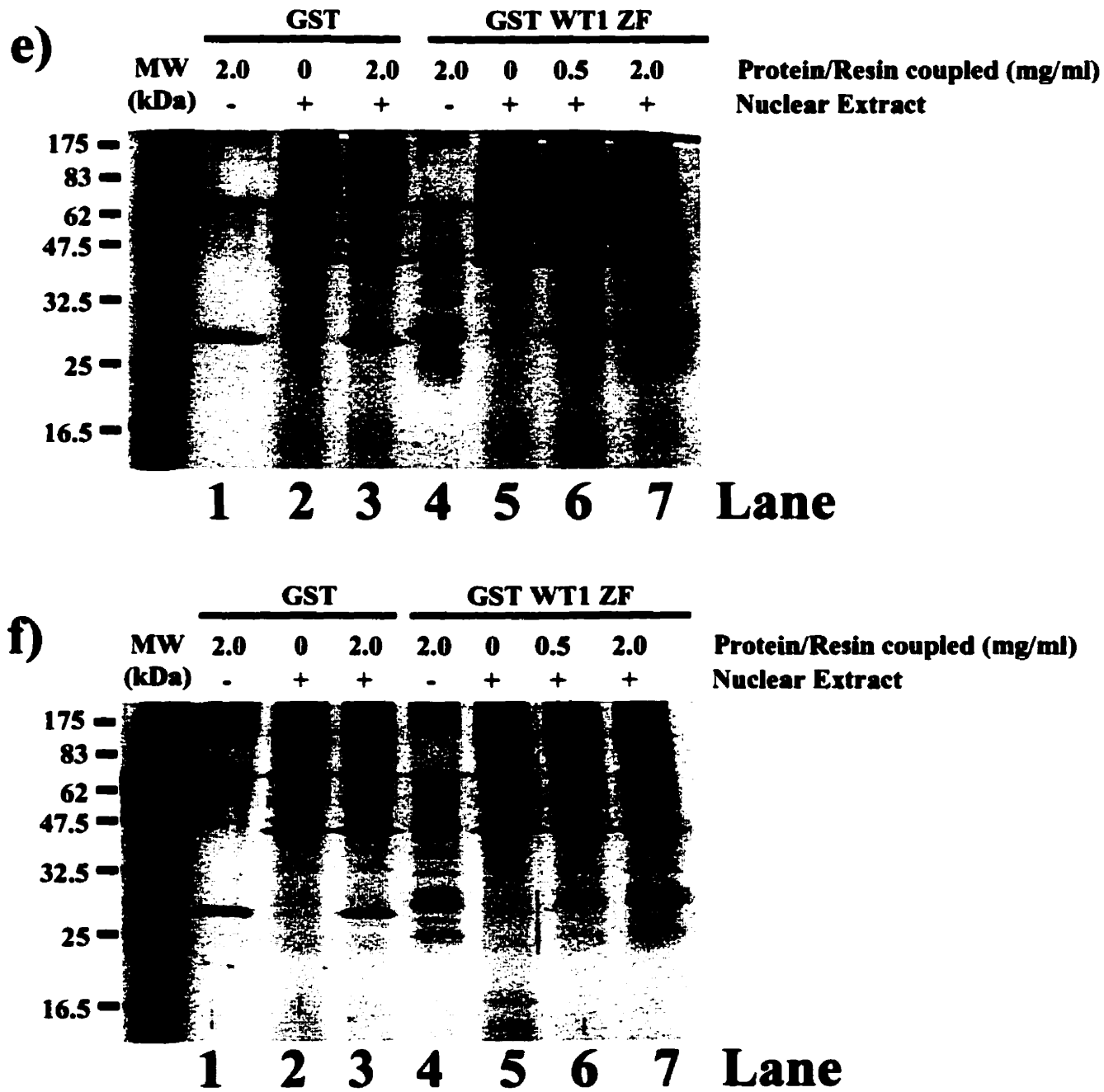
e)
GST
GST WT1 ZF
MW
(kDa)
2.0 0 2.0 2.0 0 0.5 2.0
- + + - + + +
Protein/Resin coupled (mg/ml)
Nuclear Extract
175
83
62
47.5
32.5
25
16.5
1 2 3 4 5 6 7 Lane
f)
GST
GST WT1 ZF
MW
(kDa)
2.0 0 2.0 2.0 0 0.5 2.0
- + + - + + +
Protein/Resin coupled (mg/ml)
Nuclear Extract
175
83
62
47.5
32.5
25
16.5
1 2 3 4 5 6 7 Lane

the elutions yielded similar bands as fraction 1, but with a less overall intensity (data not shown). Elutions with 1% SDS AC Buffer and SDS Sample Buffer also revealed proteins that bound non-specifically to the matrix as well as coupled proteins that had leached off the resin **(Figure 3e and f)**. Bands that appeared in the GST WT1 ZF and nuclear extract lanes **(Figure 3e and f, lanes 6 and 7)** are also present in the lanes where no GST or GST WT1 ZF fusion had been coupled **(Figure 3e and f, lanes 2 and 5)** and the lanes where GST or GST WT1 ZF fusion had been coupled but no extracts were applied **(Figure 3e and f, lanes 1 and 4)**. Proteins of approximately 62 kDa prevailed across all the lanes and probably correspond to BSA, which had been used in pre-blocking.

The 1 M NaCl AC Buffer elutions produced a singular band of approximately 32 kDa in size **(Figure 3d, lanes 6 and 7 *indicated with an arrow*)**. The high salt concentration required to elute the 32 kDa protein (1 M NaCl) suggests that it exhibits high affinity binding to WT1 ZF and since it does not appear in the elutions from the GST matrix, we conclude that it is specifically bound to WT1 ZF. This protein was excised from the gel and identified by mass spectrometry as described in the Materials and Methods.

Major peaks from the mass spectrometry were detected at 919.45, 939.52, 971.49, 1020.41, 1082.51, 1153.55, 1166.55, 1179.56, 1234.57, 1257.59, 1277.67, 1320.54, 1399.68, 1433.69, 1434.74, 1463.67, 1475.75, 1513.67, 1578.74, 1621.81, 1638.80, 1642.73, 1697.82, 1704.84, 1707.81, 1716.88, 1718.83, 1951.99, 2163.05, 2201.02, 2273.15, 2311.15, 2334.99, 2351.02, 2464.05, 2465.54, and 2550.12 Da **(Figure 4a)**. A comparison of the masses of these tryptic fragments using ProFound, a software that

Figure 4:

Identification of the 32 kDa band by mass spectrometry. The 32 kDa protein obtained from the 1 M NaCl AC Buffer elution of the affinity chromatography experiment was processed by Borealis Biosciences Inc. to produce proteolytic peptides that were then prepared for mass spectrometry with a PerCeptives Biosystems Voyager Eliete MALDI-ToF. **(a)** The mass spectrum shows high intensity peaks (indicated with their molecular masses, in Da), that were subsequently analyzed, as well as low intensity peaks that constitute the background level. This background is most likely due to various impurities present in the gel slice. ProFound search results performed on the major peaks generated from the spectrum identified our candidate protein to be either **(b)** the Bone Marrow Zinc Finger 2 protein (BMZF2 or ZNF255) or **(c)** a liver-expressed ribosomal protein S3 homologue, both of human origin. These proteins were identified by matching the observed proteolytic masses in the MALDI-ToF spectra with the hypothetical proteolytic peptide masses derived from non-redundant translated genomic databases. **(b)** For BMZF2, 8 peptides matched out of the 35 peptides measured, covering about 14% of the protein. **(c)** Six peptides matched for the ribosomal protein S3 homologue, covering approximately 24 to 30% of the protein. **(d)** For BMZF2, 7 of the 8 matched peptides correspond to the C-terminus of the zinc finger region, whereas 1 peptide matched to the N-terminus of the zinc finger region. (The zinc finger region is indicated in bold lettering.)

a)

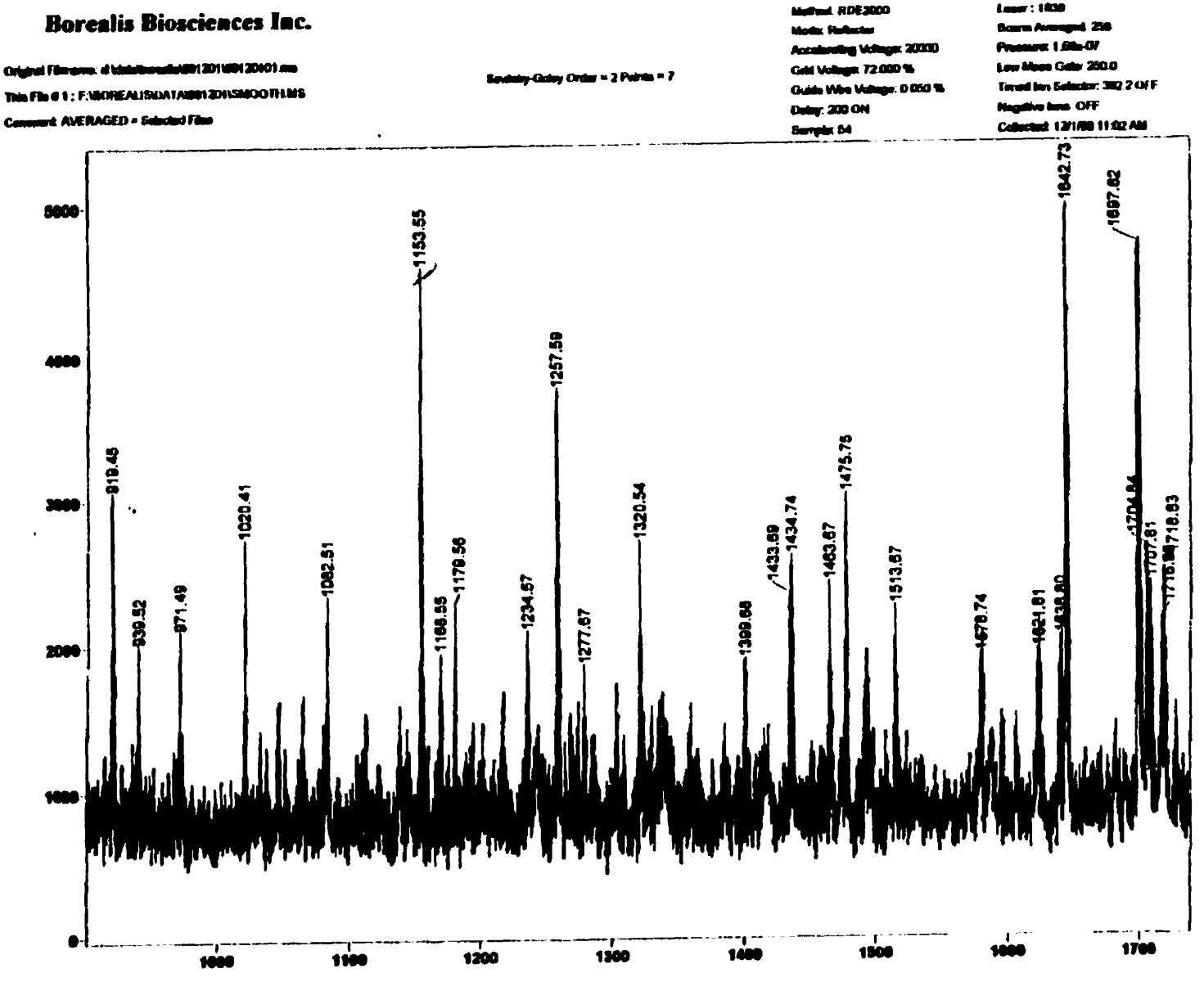
Borealis Biosciences Inc.
Original Filename: d:\data\borealis\ABI1201\ABI120401.ms
This File # 1 : F:\BOREALIS\DATA\ABI1201\SMOOTH.MS
Comment: AVERAGED = Selected Files
Savitsky-Golay Order = 2 Points = 7
Method: RDE2000
Mode: Reflector
Accelerating Voltage: 20000
Grid Voltage: 72.000 %
Guide Wire Voltage: 0.050 %
Delay: 200 ON
Samples: 64
Laser: 1838
Shots Averaged: 256
Pressure: 1.69e-07
Low Mass Gate: 250.0
Timed Ion Selector: 382.2 OFF
Negative Ions: OFF
Collected: 12/1/88 11:02 AM
5000
4000
3000
2000
1000
0
1000
1100
1200
1300
1400
1500
1600
1700
919.45
839.52
971.49
1020.41
1082.51
1153.55
1188.55
1178.56
1234.57
1257.59
1277.67
1320.54
1399.68
1433.69
1434.74
1463.67
1475.75
1513.67
1670.74
1631.81
1638.80
1642.73
1697.82
1704.84
1707.81
1718.83

Borealis Biosciences Inc.

Original Filename: d:\data\borealis\BR120\BR120101.mb

This File # 1 : F:\BOREALIS\DATA\BR120\SMOOTH M5

Comment: AVERAGED = Selected Files

Savitsky-Golay Order = 2 Points = 7

Method: RDE2000
Mode: Reflector
Accelerating Voltage: 20000
Grid Voltage: 72.000 %
Guide Wire Voltage: 0.050 %
Delay: 200 ON
Sample: 54

Laser: 1438
Scans Averaged: 256
Pressure: 1.48e-07
Low Mass Gate: 250.0
Timed Ion Selector: 382.2 OFF
Negative Ions: OFF
Collected: 12/1/99 11:02 AM

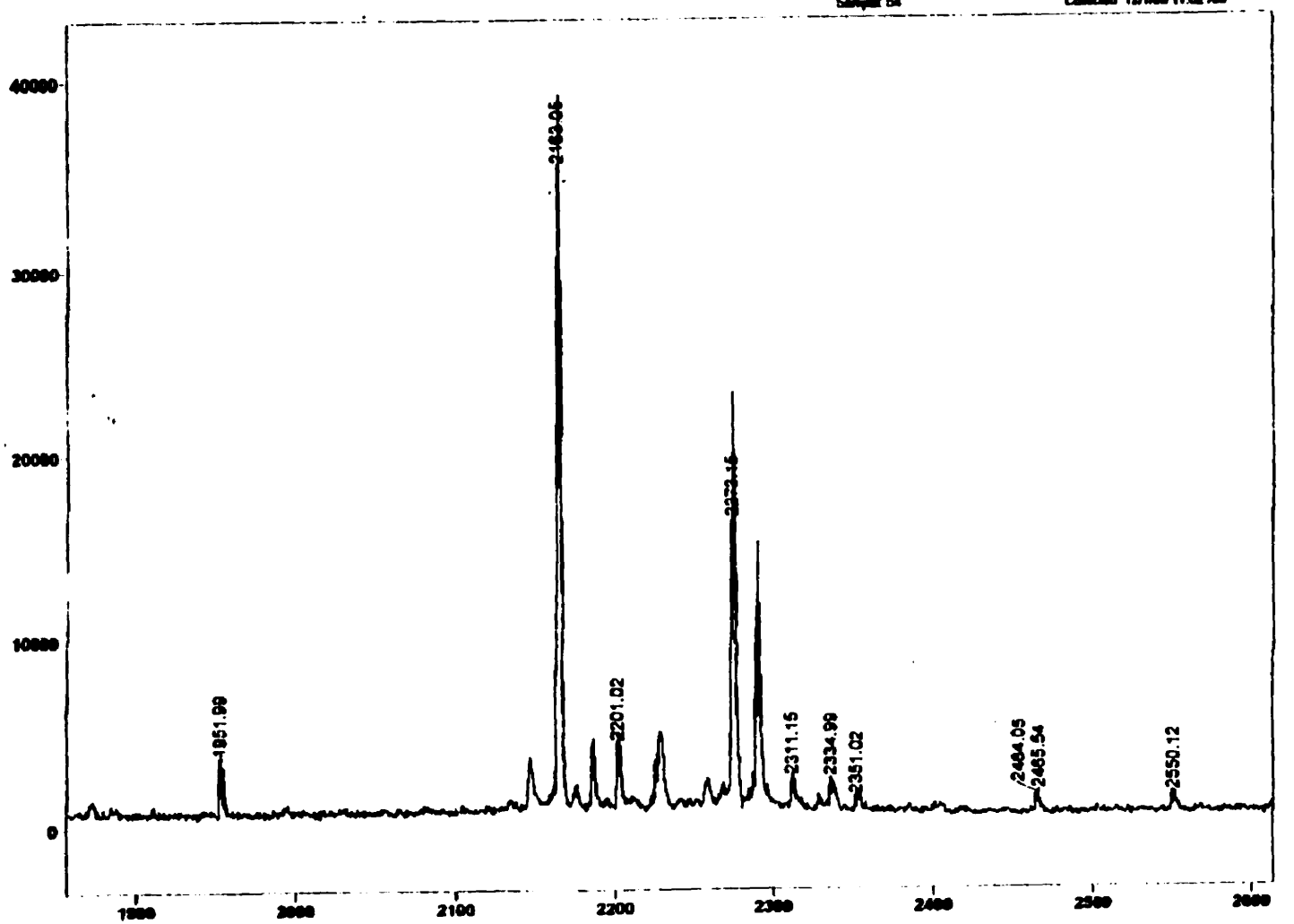

b)

Details for:

gi|5031615|ref|NP_008795.1|pBMZF2| zinc finger 2, bone marrow

gi|4884382|gb|AAD32448.1|AF067164_1 (AF067164) zinc finger protein 2 [Homo sapiens]

Sample ID : Gel 67 32 kDa [Pass:0]
Number of Measured Peptides : 38
Number of Matched Peptides : 8
Coverage of protein sequence : 14%

1167.547	M	1167.574	-0.027	464	473	0	SPGHRACLLK
1233.565	M	1233.640	-0.074	109	118	1	INQRVEHGEK
1256.586	M	1256.662	-0.076	613	623	0	LHQHVEVGEKP
1462.662	M	1462.778	-0.117	474	485	1	HGRLHSGEKPFK
1474.739	M	1474.723	0.016	421	432	1	VHIGEKPYHCEK
1637.797	M	1637.813	-0.016	492	504	1	RFTQHSQLHSHQR
1641.723	M	1641.763	-0.040	460	473	1	SCGKSFGHRACLLK
1706.802	M	1706.833	-0.031	581	594	1	LHLIHHQHVEHGEK

Miss Matched Average Masses:
2465.542 2550.119

Miss Matched Monoisotopic Masses:
919.454 939.515 971.486 1020.413 1082.513 1153.553 1179.565 1277.674 1320.540 1399.677 1433.687 1434.735 1513.673 1578.744 1621.813 1697.821 1704.835 1716.859 1718.830 1951.989 2201.023 2311.147 2334.994 2351.019 2464.046

c)

Details for:

gi|308663 (L13802) ribosomal protein small subunit [Homo sapiens]

Sample ID : Gel 67 32 kDa [Pass:0]
Number of Measured Peptides : 35
Number of Matched Peptides : 6
Coverage of protein sequence : 24-30%

918.446	M	918.517	-0.071	21	28	1	VVDPTKK
918.446	M	918.474	-0.028	36	42	0	AFAMFMIR
918.446	M	918.517	-0.071	20	27	1	KVVDPTKK
970.478	M	970.494	-0.016	137	144	0	LECVGFTK
1276.666	M	1276.702	-0.036	84	94	1	YKLITEDVQGK
1577.736	M	1577.707	0.029	95	107	0	MCLTMTHGHDLYR
1703.827	M	1703.845	-0.018	200	213	0	ACQSITFLHDVFVR
1950.981	M	1950.968	0.013	66	82	0	VFEVSLADLQMDEVAFR

Miss Matched Average Masses:
2465.542 2550.119

Miss Matched Monoisotopic Masses:
939.515 1020.413 1082.513 1153.553 1168.555 1179.565 1234.573 1257.594 1320.540 1399.677 1433.687 1434.735 1469.670 1475.747 1513.673 1621.813 1638.805 1642.731 1697.821 1707.810 1716.859 1718.830 2201.023 2311.147 2334.994 2351.019 2464.046

d)


1 METVSEAGTH QEWSFQQIWE KIASDLTRSQ DLVINSSQFS KEGDFPCQTE
51 AGLSVIHTRQ KSSQGNGYKP SFSDVSLFDF HQQLHSGEKS HTCDECGKNF
101 CYISALRIHQ RVHMGEKCYK CDVCGKEFSQ SSHLQTHQRV HTGEKPFKCV
151 ECGKGFSRRS ALNVHHKLHT GEKPYNCEEC GKAFIHDSQL QEHQRIHTGE
201 KPFKCDICGK SFCGRSRLNR HSMVHTAEKP FRCDTCDKSF RQRSALNSHR
251 MIHTGEKPYK CEECGKGFIC RRDLYTHHMV HTGEKPYNCK ECGKSFRWAS
301 CLLKHQRVHS GEKPIQCEEC GKGFYTISQC YSHQRSHSGE KPYKCVECGK
351 GYKRRLDLDF HQRVHTGEKL YNCKECGKSF SRAPCLLKHE RLHSGEKPFQ
401 CEECGKRFTQ NSHLHSHQRV HTGEKPYKCE KCGKGHNSKF NLDMHQKVHT
451 GERPYNCKEC GKSFGWASCL LKHQRLHSGE KPFKCEECGK RFTQNSQLHS
501 HQRVHTGEKP YKCDECGKGF SWSSTRLTHQ RRHSRETPLK CEQHGKNIVQ
551 NSFSEVQEKV HSVEKPYKCE DCGKGYNRRL NLDMHQRVHM GEKTWKCREC
601 DMCFSQASSL RLHQNVHVGE KP

matches the observed proteolytic masses with the hypothetical proteolytic peptide masses derived from non-redundant translated genomic databases, indicated the presence of 2 proteins: i) Bone Marrow Zinc Finger 2 (BMZF2 or ZNF255) **(Figure 4b)** and ii) a ribosomal protein, S3, homologue **(Figure 4c)**, both of human origin. Of the 35 peptides analyzed, 6 peptides matched the liver-expressed ribosomal protein S3 homologue and spanned approximately 24 - 30% of the protein. For BMZF2, 8 peptides matched out of the 35 peptides measured, covering about 14% of the protein. Seven of the 8 peptides correspond to the C-terminal end of the zinc finger region, whereas 1 peptide corresponds to the N-terminus of the zinc finger region **(Figure 4d)**.

Given that WT1 is a nuclear protein, whereas mature ribosomal proteins are generally found in the cytoplasm, a putative interaction between WT1 and ribosomal protein S3 homologue was not investigated at this time. For the purpose of the studies described herein, we focussed on defining a potential interaction between WT1 and BMZF2.

Cloning and Sequencing of BMZF2 cDNA

BMZF2 is an approximately 70 kDa protein containing of a small N-terminus region bearing homology to the KRAB motif. The KRAB (Kruppel associated box) motif is highly conserved in Kruppel-like zinc finger proteins and is capable of mediating transcriptional repression (120). BMZF2 also contains 18 Kruppel-like zinc fingers at the C-terminus (121) **(Figure 5)**. *BMZF2* is expressed in all cells of the hematopoietic lineage including most leukemia cells. The *BMZF2* cDNA was originally cloned and

Figure 5:

BMZF2 (a) mRNA and (b) protein structures. BMZF2 mRNA is 3003 bp in length with a large 5'UTR of about 1 kb. It has an ORF of 1866 bp, which encodes a protein of 622 amino acids. The BMZF2 protein has 18 tandem zinc fingers and a novel N-terminal domain named Kruppel-related novel box (KRNB). The KRNB domain is rich in hydrophobic amino acids (Gly, Ile, Ala, Leu, and Phe) and negatively charged amino acids (Asp) that are characteristic of transcription factors. The amino acid knuckle, TGE(R/K)P(F/Y)X (where X represents any amino acid), which is highly conserved in Kruppel-like zinc finger genes, is found between the zinc finger motifs of BMZF2. The ZnF UBP, LIM, and C1 domains predicted by SMART analysis have also been indicated.

a)

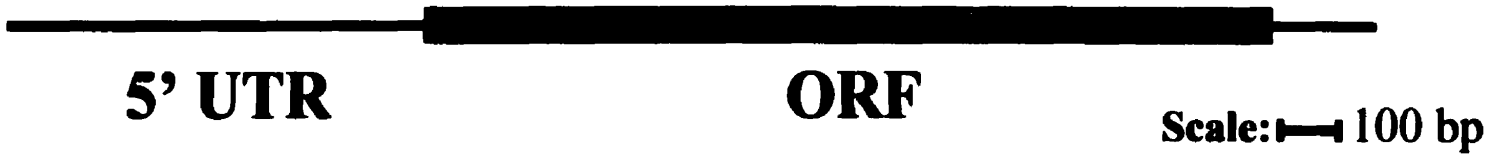
5' UTR
ORF
Scale: 100 bp

b)

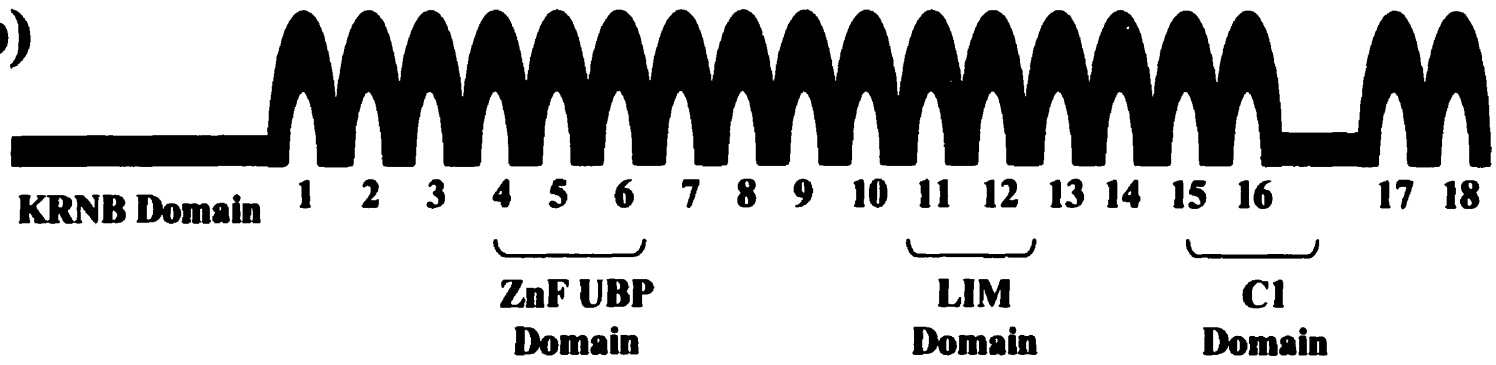
KRNB Domain
1 2 3 4 5 6 7 8 9 10 11 12 13 14 15 16 17 18
ZnF UBP Domain
LIM Domain
C1 Domain

characterized by Han et. al (121). They reported the sequence of a cDNA of 3006 bp containing a large 5'UTR of about 1 kb and an ORF of 1869 bp, encoding a protein of 623 amino acids. To obtain a cDNA clone of BMZF2, we designed primers corresponding to the 5' and 3' ends of the ORF and cloned this portion of the cDNA by RT-PCR from HeLa cell mRNA. An RT-PCR product of approximately 2 kb was obtained **(Figure 6)** and cloned into pKSII+ vector for DNA sequencing using the Sanger method (119,122).

We noted discrepancies between the sequence of our cDNA and the reported sequence (121). Sequencing directly from the PCR product demonstrated that these nucleotide differences were not due to mistakes generated during the RT-PCR amplification steps **(Figure 7a)**. The differences lie in the N-terminus region where instead of 2 adenines at positions 153 and 154 and 192 and 193 or 2 thymidines at positions 200 and 201, as reported by Han et al. (121), we find only one adenine at positions 153 and 192 (or revised, 191) and one thymidine at position 200 (or revised, 198) **(Figure 7b)**. The occurrence of three such discrepancies in the N-terminus region alters the reading frame (and hence amino acid sequence) bracketed by the outermost discrepancies and shortens the N-terminus region by 1 amino acid overall to 80 amino acids. This change, however, does not alter the reading frame, or the amino acid sequence, of the zinc finger domain of BMZF2. BMZF2, therefore, has an ORF of 1866 bp which would encode a protein of 622 amino acids.

Figure 6:

RT-PCR product of BMZF2 mRNA ORF. Based on the sequence submitted by Han et al. (121) to GenBank, we designed primers corresponding to the 5' and 3' ends of the predicted ORF to amplify this region from HeLa cell cDNA. An RT-PCR product of approximately 2 kb was obtained (expected size 1869 bp) as shown by electrophoresis on a 1% agarose gel stained with ethidium bromide.

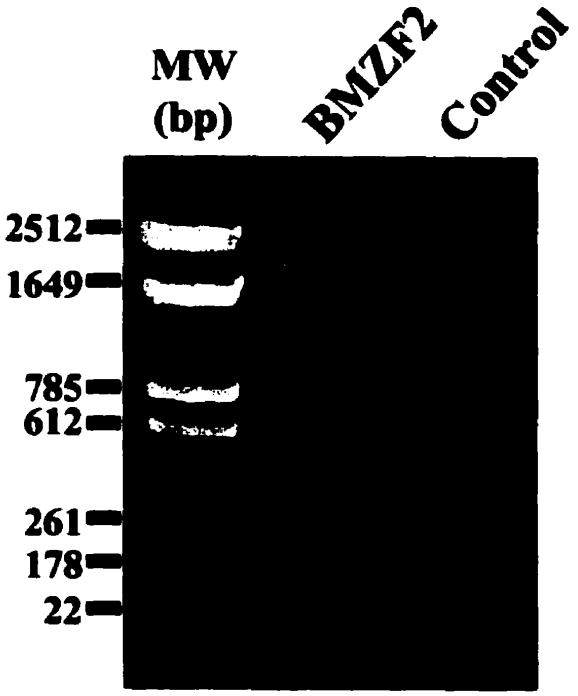
MW
(bp)
BMZF2
Control
2512
1649
785
612
261
178
22

Figure 7:

Nucleotide and amino acid sequences of the BMZF2 KRNB domain. There were discrepancies between the sequencing results we obtained and the sequence reported by Han et al. (121). **(a)** Sequencing directly from the PCR product demonstrated that these nucleotide differences were not due to mistakes generated during the RT-PCR amplification steps. We read one adenine at positions 153 and 192 (or revised, 191) and one thymidine at position 200 (or revised, 198) (indicated with arrows). **(b)** Instead of 2 adenines at positions 153 and 154 and 192 and 193 and 2 thymidines at positions 200 and 201 for the sequence that is reported in the GenBank (GenBank Accession #: AF067164), we read one adenine at positions 153 and 192 (or revised, 191) and one thymidine at position 200 (or revised, 198) (upper panel, indicated with bold lettering). The occurrence of three such discrepancies in the N-terminus region alters the reading frame (and hence the amino acid sequence) bracketed by the outermost discrepancies (boxed and shaded in grey), and shortens the N-terminus region by 1 amino acid overall to 80 amino acids (lower panel). This change, however, does not alter the reading frame, or the amino acid sequence, of the zinc finger domain of BMZF2. BMZF2 cDNA, therefore, has an ORF of 1866 bp which would encode a protein of 622 amino acids.

a)

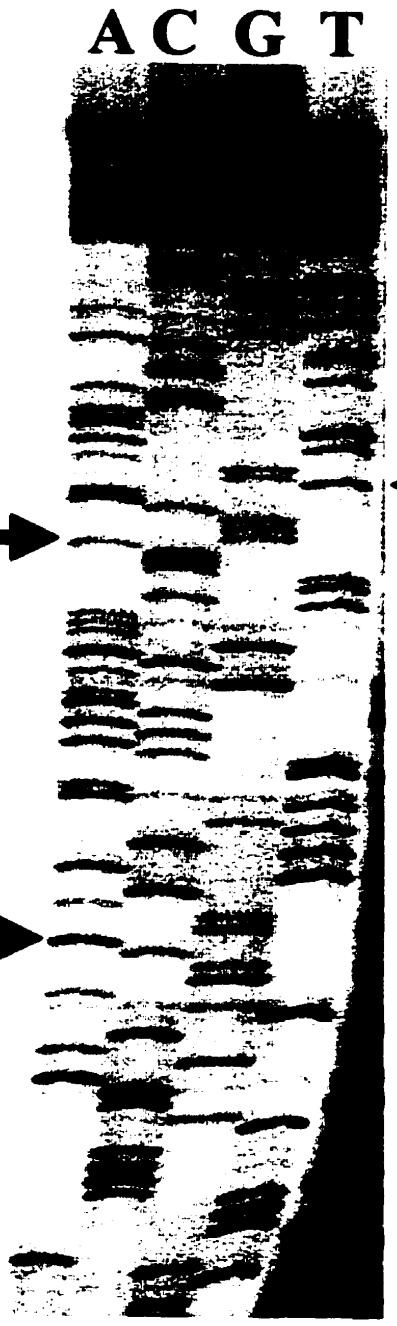
A C G T
T nucleotide 200
(or revised, 198)
nucleotide 192
(or revised, 191)
A
nucleotide 153
A

b) Sequence Reported by Han et al.

```
1   ATG GAG ACT GTT TCA GAA GCA GGA ACA CAT CAA GAG TGG TCC TTC CAG CAA ATC TGG
1   met glu thr val ser glu ala gly thr his gln glu trp ser phe gln gln ile trp

58  GAA AAA ATT GCA AGT GAT TTA ACC AGG TCT CAA GAC TTG GTG ATA AAT AGC TCT CAG
20  glu lys ile ala ser asp leu thr arg ser gln asp leu val ile asn ser ser gln

115 TTC TCC AAA GAA GGT GAT TTC CCC TGC CAG ACT GAG GCA AGG ACT ATC TGT AAT TCA
39  phe ser lys glu gly asp phe pro cys gln thr glu ala arg thr ile cys asn ser

172 CAC AAG ACA GAA ATC TTC CCA AGG GCA ATT GGA TAT AAA CCA TCC TTC AGT GAT GTC
58  his lys thr glu ile phe pro arg ala ile gly tyr lys pro ser phe ser asp val

229 TCC CTC TTT GAT TTT
77  ser leu phe asp phe
```

Revised Sequence Based on Our Sequencing Results

```
1   ATG GAG ACT GTT TCA GAA GCA GGA ACA CAT CAA GAG TGG TCC TTC CAG CAA ATC TGG
1   met glu thr val ser glu ala gly thr his gln glu trp ser phe gln gln ile trp

58  GAA AAA ATT GCA AGT GAT TTA ACC AGG TCT CAA GAC TTG GTG ATA AAT AGC TCT CAG
20  glu lys ile ala ser asp leu thr arg ser gln asp leu val ile asn ser ser gln

115 TTC TCC AAA GAA GGT GAT TTC CCC TGC CAG ACT GAG GCA GGA CTA TCT GTA ATT CAC
39  phe ser lys glu gly asp phe pro cys gln thr glu ala gly leu ser val ile his

172 ACA AGA CAG AAA TCT TCC CAG GGC AAT GGA TAT AAA CCA TCC TTC AGT GAT GTC TCC
58  thr arg gln lys ser ser gln gly asn gly tyr lys pro ser phe ser asp val ser

229 CTC TTT GAT TTT
77  leu phe asp phe
```

Bioinformatics Analysis of BMZF2

BLAST searches were performed on the BMZF2 N-terminus and full-length amino acid sequences. The results indicated that the BMZF2 N-terminus shared a 32% homology over 73 amino acids with the N-terminus of Zinc Finger Protein 45 (ZN45 or BRC1744) (GenBank accession no. Q02386). ZN45 is a nuclear protein which contains an N-terminal KRAB box and 15 Kruppel-like zinc fingers at its C-terminus. It is likely that ZN45 functions as a transcription factor or a nucleic acid binding protein. The full-length BMZF2 protein shows approximately 50% homology to Zinc Finger Protein 91 (ZN91). ZN91 is an uncharacterized protein whose gene maps to chromosomal region 19p12.

Protein sequence analysis using the Simple Modular Architecture Research Tool (SMART), a web-based analysis tool, indicated that the BMZF2 protein harbors some potentially interesting domains **(Figure 5)**. As expected, SMART predicted that BMZF2 has 18 zinc fingers. Upon closer inspection, it is apparent that the first 16 zinc fingers exist together in a tandem array, followed by a linker region approximately the length of one zinc finger, and terminating with two zinc fingers. SMART also predicted three domains that are "hidden" within the zinc finger region. These are the ZnF UBP domain (amino acids 192 to 251), the LIM domain (amino acids 372 to 432), and the C1 domain (amino acids 499 to 541). LIM domains were first recognized in 3 homeodomain proteins and named for them: *c.elegans* LIN-11, rat ISL1, and *c. elegans* MEC-3 (123). The LIM domain is a zinc-binding domain that has a role as a mediator of protein-protein interactions via tyrosine-containing motifs. LIM domains are found in many key

regulators of developmental pathways, such as LHX1 (124) and LMO2 (125). The C1 domain stands for "protein kinase C conserved region 1" and is very cysteine-rich. Some C1 domains bind phorbol esters and diacylglycerol while others bind RasGTP. C1 domains also bind zinc. C1 domains have been found in protein kinase C (126) and the Raf-1 protein (127). The function of the ZnF UBP domain (Ubiquitin Carboxyl-terminal Hydrolase-like zinc finger) is not very well defined but this domain has been found in ubiquitin carboxyl-terminal hydrolase 5 (128) and histone deacetylase 6 (129).

WT1 Interacts with BMZF2 in vitro

We verified the interaction between BMZF2 and WT1 in vitro by performing GST pulldown assays. GST WT1 ZF protein was bound to glutathione sepharose 4B resin and incubated with in vitro translated BMZF2 protein to assess binding. GST coupled to glutathione sepharose served as a control for non-specific binding. In vitro translated p53 protein served as a positive control for the binding assay. After a series of washes, the resin was eluted with SDS Sample Buffer and the elutions were analyzed by SDS-PAGE and autoradiography of the dried gels.

Gel 1 showed 20% of the flowthrough in each lane **(Figure 8a)**. Gel 2 showed that there were no bands present in the GST lanes **(Figure 8b, lanes 1 and 2)**. This indicated that the interactions we observed in the GST WT1 ZF lanes were not due to non-specific interactions with GST. A band of approximately 53 kDa in the GST WT1 ZF and p53 lane **(Figure 8b, lane 4)** indicated that p53 bound to WT1 ZF, as expected of the positive control. A band of approximately 70 kDa in the GST WT1 ZF and BMZF2

Figure 8:

WT1 interacts with BMZF2 in vitro. GST pulldown assays were carried out to verify the interaction between BMZF2 and WT1 in vitro. Purified GST WT1 ZF proteins were bound to glutathione sepharose 4B resin and then incubated with in vitro translated ^{35}S-labelled BMZF2 protein to assess binding. After a series of washes, the resin was eluted with SDS Sample Buffer and the elutions were analyzed by SDS-PAGE and autoradiography of the dried gels. **(a)** 20% of the flowthrough is shown in each lane. **(b)** GST coupled to glutathione sepharose served as a control for non-specific binding. There were no bands present in the GST lanes (lanes 1 and 2) which indicated that the interactions we observed in the GST WT1 ZF lanes were not due to non-specific interactions with GST. A band of approximately 53 kDa in the GST WT1 ZF and p53 lane (lane 4) indicated that p53 bound to WT1 ZF, as expected of the positive control. A band of approximately 70 kDa in the GST WT1 ZF and BMZF2 lane (lane 3) indicated that there was binding between WT1 and BMZF2. Proteins of approximately 42 and 58 kDa also observed in this lane probably correspond to degradation products of the in vitro translated BMZF2.

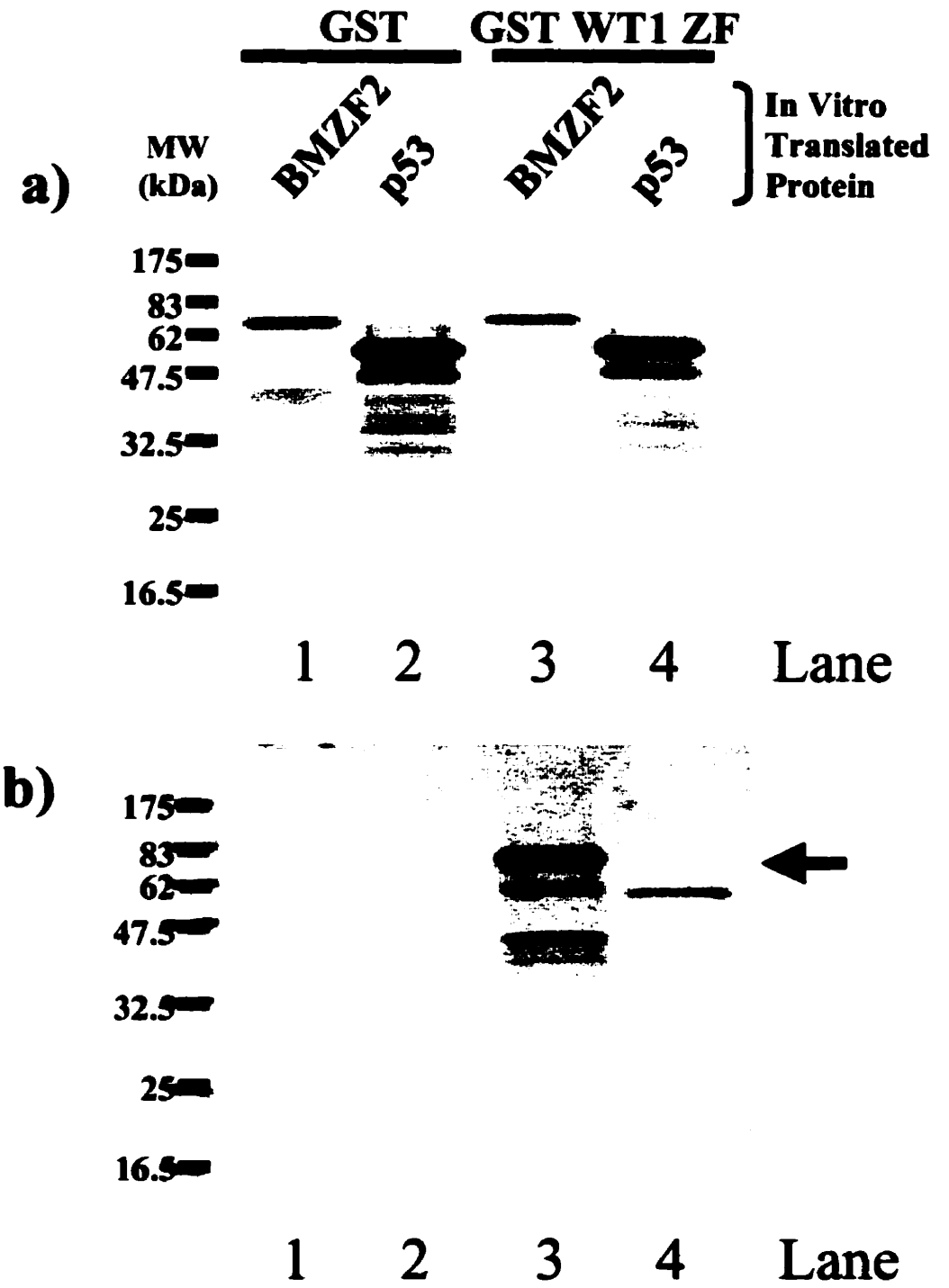
a)
GST
GST WT1 ZF
BMZF2
p53
BMZF2
p53
In Vitro Translated Protein
MW (kDa)
175
83
62
47.5
32.5
25
16.5
1 2 3 4 Lane
b)
175
83
62
47.5
32.5
25
16.5
1 2 3 4 Lane

lane **(Figure 8b, lane 3)** indicated that there was binding between WT1 and BMZF2. Proteins of approximately 42 and 58 kDa also observed in this lane probably correspond to degradation products of the in vitro translated BMZF2.

DISCUSSION

Utilizing affinity chromatography and mass spectrometry analysis, we have identified a new potential WT1 (–KTS) interacting protein, BMZF2. ProFound Search results indicated that 8 out of the 35 tryptic peptides measured matched closely to the computed masses of the BMZF2 tryptic peptides, with negligible error **(Figure 4b)**. Masses of peptides from a proteolytic digestion of a protein are compared to the masses of a peptide database calculated from the National Center for Biotechnology Information (NCBI) non-redundant protein database. The NCBI GenBank database has increased in size, from 4,864,570 sequences in December 1999, when the ProFound Search was carried out, to 7,077,491 sequences as of August 2000 (130). If BMZF2 was not the correct match, the likelihood of not finding the correct match is ~ 31%, representing the proportion of sequences in the database that have not been searched.

BMZF2

BMZF2 is a zinc finger gene expressed in the hematopoietic system (121). The cDNA was originally cloned by Han et al. (121) from normal bone marrow mRNA and a leukemia cell line as part of their efforts to explore the molecular regulation of hematopoiesis. They identified 6 novel genes all containing tandemly repeated Kruppel-like Cys_2/His_2 zinc fingers at the C-terminus with possible transcriptional regulatory elements, such as the KRAB domain and the SCAN box, at the N-terminus. One of these genes was *BMZF2* (or ZNF255).

The BMZF2 protein has 18 tandem zinc fingers and a novel N-terminal domain named Kruppel-related novel box (KRNB) (121) **(Figure 5)**. The KRNB domain is rich

in hydrophobic amino acids (Gly, Ile, Ala, Leu, and Phe) and negatively charged amino acids (Asp) that are characteristic of transcription factors. The amino acid knuckle, TGE(R/K)P(F/Y)X (where X represents any amino acid), which is highly conserved in Kruppel-like zinc finger genes, is found between the zinc finger motifs of BMZF2 (131). Therefore, it was reasonable to predict that BMZF2 could encode a nucleic acid-binding protein with transcriptional regulatory properties.

BMZF2 is expressed ubiquitously in the cells of the hematopoietic lineage and is selectively expressed in other tissues (121). Han et al. (121) examined the expression pattern of *BMZF2* in various tissues and leukemia cell lines by semi-quantitative RT-PCR, as the low expression levels of this gene are undetectable using Northern blot analysis. There is very low expression in the heart, lung, and liver and slightly higher expression in the brain, kidney, testis, spleen, pancreas, stomach, and placenta (121).

BMZF2 is also expressed in the HeLa cell line, a cervical cancer cell line. Since we cloned the BMZF2 cDNA by RT-PCR from HeLa cell mRNA and the nuclear extracts used for the affinity chromatography experiment were prepared from HeLa cells as well, *BMZF2* transcripts and protein are both expressed in HeLa cells. We have not investigated the abundance of the WT1 and BMZF2 proteins within the HeLa cell line and it is possible that the expression of either may be upregulated in tumor cells.

BMZF2 is a Potential Interacting Protein of WT1 (-KTS)

The results we obtained from the Affinity Chromatography and GST pulldown experiments suggest that there is binding between the WT1 (–KTS) zinc fingers and the

70 kDa BMZF2 protein. We are attempting to further characterize this interaction in vivo by using a mammalian expression system and transfecting into cultured cells.

We note that although the conceptual translation of BMZF2 predicts a protein of 70 kDa, initially a polypeptide of ~32 kDa was identified **(Figure 3d, lanes 6 and 7)**. We then wondered if this could be the result of BMZF2 degradation in vivo. This hypothesis was supported by the mass spectrometry results of the 32 kDa band, which showed that 7 out of the 8 peptides matched correspond to the C-terminus of BMZF2, whereas 1 peptide corresponds to the N-terminus of the zinc finger region **(Figure 4d)**. The 7 C-terminal peptides can be placed on a contiguous 32 kDa BMZF2 proteolytic fragment. It is possible that the 32 kDa band is the product of BMZF2 degradation in vivo and corresponds to either a C-terminus fragment of the BMZF2 zinc finger region or a more N-terminal fragment. To verify whether or not the protein was being degraded in vivo from the N-terminus, BMZF2 can be tagged at the C-terminus and cellular extracts can be analyzed by Western blotting using antibodies against the tag.

Zinc Fingers Can Mediate Protein-Protein Interactions

It has been estimated that approximately 500 zinc finger proteins are encoded by the yeast genome and that approximately 1% of all mammalian genes encode zinc finger proteins (132). While zinc finger motifs are commonly known for their DNA and RNA-binding abilities, recent reports suggest that zinc finger proteins can also mediate protein-protein interactions. This might help to explain the prevalence of these proteins within the cell.

The Ikaros protein, which plays a central role in the development of lymphoid cells, provides a good example of a zinc finger protein that is capable of mediating DNA-binding and protein-protein interaction (133). Ikaros contains up to 6 Kruppel-like fingers (depending on splicing patterns), with the first four involved in sequence-specific DNA binding and the last two involved in Ikaros homodimerization. The two C-terminal zinc fingers are conserved in all splicing isoforms. Aiolos, another zinc finger protein, interacts with both Ikaros and itself through its own double-finger dimerization domain (134). Dimerization of Ikaros and Aiolos modulates their ability to bind DNA and to activate transcription.

Kruppel-like zinc fingers can also make contact with the finger proteins from other families. For example, the GATA-1 protein, which contains two Cys_2/Cys_2 fingers, reserves its C-terminal finger for DNA binding while it interacts through its N-terminal finger with finger 6 of FOG (Friend of GATA), which exhibits a Kruppel-related Cys_2/His/Cys configuration and appears to be somewhat isolated from FOG's other 8 fingers (135). DNA binding by Kruppel-like zinc fingers requires a tandem array of fingers (136) and it has been suggested that the isolation of one or a few fingers may serve as an indication of their non-DNA-binding function (132).

Furthermore, the Kruppel-like zinc fingers of the transcription factors Sp1 and EKLF appear to be capable of binding both DNA and proteins simultaneously (137). It has been suggested that the interaction between DNA-bound Sp1, EKLF, FOG, and GATA could facilitate communication between widely-spaced control elements in DNA. This is further complicated by the observation that both fingers of GATA-1 are

implicated in homodimerization or even multimerization and that GATA-1 can dimerize while bound to DNA (138).

Most nuclear zinc finger proteins contain multiple zinc fingers, while the cytoplasmic zinc finger proteins often contain only one or two (132). One possible explanation for this is that the tandem array of fingers is usually required for high-affinity and sequence-specific binding to DNA, whereas in many cases, single fingers may be sufficient for interacting with other proteins, which typically present more heterogeneous surfaces.

We have not identified the domains of interaction, which can be determined by performing GST pulldown experiments with WT1 zinc finger and BMZF2 truncation mutants. Of greater interest to us is the effect of the interaction between the WT1 (–KTS) protein, a known tumor suppressor gene and transcription factor, and the BMZF2 protein, a potential transcription factor. We would like to understand whether or not there is a physiological or pathological effect as a result of the interaction.

Physiological and Pathological Expression of *WT1* in Hematopoiesis

WT1 expression has been detected in fetal spleen, liver, and thymus. These are all tissues in which hematopoiesis takes place during embryonic development (1). *WT1* transcripts have also been detected in adult bone marrow, lymph nodes, and peripheral blood. There is data to suggest that WT1 may play a role in the development of erythroid, myeloid, and lymphoid cells during fetal and adult stages. *WT1* expression is found predominantly in more immature cells and differentiation of these cells is

correlated with downregulation of *WT1* expression. This suggests that WT1 has a role in early hematopoiesis (139-141).

While *WT1* is only transiently expressed in normal hematopoiesis, it is continuously expressed at high levels in acute myelocytic and lymphocytic leukemia and in chronic myelocytic leukemia (142). A high level of *WT1* expression in leukemia cells is linked to poor prognosis in patients with leukemia, rendering the *WT1* gene a novel marker for leukemia cells (143). Assays of the *WT1* mRNA level have also become a rapid way to assess the effectiveness of treatment and to evaluate the degree of eradication of leukemic cells in leukemia patients. Conversely, the loss of *WT1* gene function has also been implicated in the development of malignancies including acute leukemias (144). This correlates with the tumor suppressive effects of *WT1* expression in leukemia cell lines and suggests that *WT1* acts as a differentiation-promoting gene during hematopoiesis and that the loss of functional *WT1* expression may contribute to leukemogenesis in vivo.

What then is the relationship between WT1 and BMZF2 in hematopoiesis and leukemogenesis? Perhaps, WT1 regulates the expression of the potential transcription factor, BMZF2, in hematopoiesis. Since *BMZF2* transcripts are detected in all cells of the hematopoietic lineage, WT1 may regulate BMZF2's activity through protein-protein interactions, or conversely, BMZF2 may regulate WT1's activity.

Mammalian Kruppel-like Zinc Fingers

Mammalian Kruppel-like zinc finger genes are usually involved in embryo development and hematopoiesis. The KRAB domain was found to be evolutionarily conserved in approximately one-third of these zinc finger proteins, and while it normally functions as a transcriptional repressor (120), another domain which has also been found associated with Cys_2/His_2 zinc fingers, the SCAN box, functions as a potent transactivator (145).

An example of a Kruppel-like zinc finger protein that is involved in the physiological and pathological regulation of hematopoiesis is the Erythroid Kruppel-like Factor (EKLF). EKLF, which regulates the expression of the β–globin gene in vivo (146,147), is a protein of 362 amino acids that contains three C-terminal zinc fingers (148). The EKLF gene is localized to chromosome 19p13, a region which is deleted in some cases of acute erythroleukemia, but very rarely deleted in other acute leukemia subtypes (149). The loss of chromosomal region 19p in certain cases of erythroleukemia is consistent with the tumor suppressor role of EKLF. In addition, the re-introduction of other members of the Kruppel-like factor family is associated with a loss of proliferation and/or differentiation; for example, the expression of the *WT1* gene will result in growth inhibition (7). Interestingly, the zinc fingers of WT1 are related to Cys_2/His_2 zinc fingers of EKLF, which also contains a proline-rich N-terminus.

Summary

We have isolated and identified a new potential WT1-interacting protein, BMZF2, which binds the zinc finger region of the WT1 (–KTS) isoform. Amino acid sequence

analysis of BMZF2 suggests that it is a potential transcription factor with DNA-binding abilities. WT1 is a known tumor suppressor gene and transcription factor. The expression patterns of BMZF2 and WT1 suggest that they are both important, if not crucial, to the regulation of mammalian development and hematopoiesis. Clearly, additional work is required to better understand the nature of the WT1-BMZF2 interaction as well as the physiological and pathological effects that may result.

REFERENCES

1. **Menke, A.L., A.J. van der Eb, and A.G. Jochemsen.** 1998. The Wilms' tumor 1 gene: oncogene or tumor suppressor gene?. [Review] [252 refs]. International Review of Cytology **181**:151-212.

2. **Matsunaga, E.** 1982. Cancer susceptibility: family studies of retinoblastoma and Wilms tumor. Progress in Clinical & Biological Research **103 Pt B**:241-249.

3. **Breslow, N.E. and B. Langholz.** 1983. Childhood cancer incidence: geographical and temporal variations. International Journal of Cancer **32**:703-716.

4. **Machin, G.A.** 1980. Persistent renal blastema (nephroblastomatosis) as a frequent precursor of Wilms' tumor; a pathological and clinical review. Part 2. Significance of nephroblastomatosis in the genesis of Wilms' tumor. American Journal of Pediatric Hematology-Oncology **2**:253-261.

5. **Gubler, M.C., Y. Yang, C. Jeanpierre, S. Barbaux, and P. Niaudet.** 1999. WT1, renal development, and glomerulopathies. [Review] [90 refs]. Advances in Nephrology From the Necker Hospital **29**:299-315.

6. **Call, K.M., C.Y. Ito, C. Lindberg, A. Memisoglu, C. Petrou, T. Glaser, C. Jones, and D.E. Housman.** 1992. Mapping and characterization of 129 cosmids on human chromosome 11p. Somatic Cell & Molecular Genetics **18**:463-475.

7. **Hastie, N.D.** 1993. Wilms' tumour gene and function. [Review] [44 refs]. Current Opinion in Genetics & Development **3**:408-413.

8. **Pelletier, J., W. Bruening, C.E. Kashtan, S.M. Mauer, J.C. Manivel, J.E. Striegel, D.C. Houghton, C. Junien, R. Habib, and L. Fouser.** 1991. Germline mutations in the Wilms' tumor suppressor gene are associated with abnormal urogenital development in Denys-Drash syndrome. Cell **67**:437-447.

9. **Pelletier, J., W. Bruening, F.P. Li, D.A. Haber, T. Glaser, and D.E. Housman.** 1991. WT1 mutations contribute to abnormal genital system development and hereditary Wilms' tumour. Nature **353**:431-434.

10. **Haber, D.A., S. Park, S. Maheswaran, C. Englert, G.G. Re, D.J. Hazen-Martin, Sens, DA, and A.J. Garvin.** 1993. WT1-mediated growth suppression of Wilms tumor cells expressing a WT1 splicing variant. Science **262**:2057-2059.

11. **Kreidberg, J.A., H. Sariola, J.M. Loring, M. Maeda, Pelletier, D. Housman, and R. Jaenisch.** 1993. WT-1 is required for early kidney development. Cell **74**:679-691.

12. **Birchmeier, C., D. Meyer, and D. Riethmacher**. 1995. Factors controlling growth, motility, and morphogenesis of normal and malignant epithelial cells. [Review] [280 refs]. International Review of Cytology **160**:221-266.

13. **Armstrong, J.F., K. Pritchard-Jones, W.A. Bickmore, N.D. Hastie, and J.B. Bard**. 1993. The expression of the Wilms' tumour gene, WT1, in the developing mammalian embryo. Mechanisms of Development **40**:85-97.

14. **Pritchard-Jones, K. and S. Fleming**. 1991. Cell types expressing the Wilms' tumour gene (WT1) in Wilms' tumours: implications for tumour histogenesis. Oncogene **6**:2211-2220.

15. **Kent, J., A.M. Coriat, P.T. Sharpe, N.D. Hastie, and H. Van, V.** 1995. The evolution of WT1 sequence and expression pattern in the vertebrates. Oncogene **11**:1781-1792.

16. **Rackley, R.R., A.M. Flenniken, N.P. Kuriyan, P.M. Kessler, M.H. Stoler, Williams, and BR**. 1993. Expression of the Wilms' tumor suppressor gene WT1 during mouse embryogenesis. Cell Growth & Differentiation **4**:1023-1031.

17. **Barbaux, S., P. Niaudet, M.C. Gubler, J.P. Grunfeld, F. Jaubert, F. Kuttenn, C.N. Fekete, N. Souleyreau-Therville, E. Thibaud, M. Fellous, and K. McElreavey**. 1997. Donor splice-site mutations in WT1 are responsible for Frasier syndrome. Nature Genetics **17**:467-470.

18. **Kikuchi, H., A. Takata, Y. Akasaka, R. Fukuzawa, H. Yoneyama, Y. Kurosawa, M. Honda, Y. Kamiyama, and J. Hata**. 1998. Do intronic mutations affecting splicing of WT1 exon 9 cause Frasier syndrome? Journal of Medical Genetics **35**:45-48.

19. **Park, S., M. Schalling, A. Bernard, S. Maheswaran, G.C. Shipley, D. Roberts, J. Fletcher, R. Shipman, J. Rheinwald, and G. Demetri**. 1993. The Wilms tumour gene WT1 is expressed in murine mesoderm-derived tissues and mutated in a human mesothelioma. Nature Genetics **4**:415-420.

20. **Ladanyi, M. and W. Gerald**. 1994. Fusion of the EWS and WT1 genes in the desmoplastic small round cell tumor. Cancer Research **54**:2837-2840.

21. **King-Underwood, L., J. Renshaw, and K. Pritchard-Jones**. 1996. Mutations in the Wilms' tumor gene WT1 in leukemias. Blood **87**:2171-2179.

22. **Fabre, A., A.H. McCann, D. O'Shea, D. Broderick, G. Keating, B. Tobin, T. Gorey, and P.A. Dervan**. 1999. Loss of heterozygosity of the Wilms' tumor suppressor gene (WT1) in in situ and invasive breast carcinoma. Human Pathology **30**:661-665.

23. **Silberstein, G.B., K. Van Horn, P. Strickland, C.T.J. Roberts, and C.W. Daniel.** 1997. Altered expression of the WT1 wilms tumor suppressor gene in human breast cancer. Proceedings of the National Academy of Sciences of the United States of America **94**:8132-8137.

24. **Gessler, M., A. Konig, and G.A. Bruns.** 1992. The genomic organization and expression of the WT1 gene. Genomics **12**:807-813.

25. **Pavletich, N.P. and C.O. Pabo.** 1991. Zinc finger-DNA recognition: crystal structure of a Zif268-DNA complex at 2.1 A. Science **252**:809-817.

26. **Rauscher, F.J., J.F. Morris, O.E. Tournay, D.M. Cook, and Curran.** 1990. Binding of the Wilms' tumor locus zinc finger protein to the EGR-1 consensus sequence. Science **250**:1259-1262.

27. **Madden, S.L., D.M. Cook, and F.J. Rauscher.** 1993. A structure-function analysis of transcriptional repression mediated by the WT1, Wilms' tumor suppressor protein. Oncogene **8**:1713-1720.

28. **Reddy, J.C., J.C. Morris, J. Wang, M.A. English, D.A. Haber, Y. Shi, and J.D. Licht.** 1995. WT1-mediated transcriptional activation is inhibited by dominant negative mutant proteins. Journal of Biological Chemistry **270**:10878-10884.

29. **Englert, C., M. Vidal, S. Maheswaran, Y. Ge, R.M. Ezzell, K.J. Isselbacher, and D.A. Haber.** 1995. Truncated WT1 mutants alter the subnuclear localization of the wild-type protein. Proceedings of the National Academy of Sciences of the United States of America **92**:11960-11964.

30. **Wang, Z.Y., Q.Q. Qiu, M. Gurrieri, J. Huang, and T.F. Deuel.** 1995. WT1, the Wilms' tumor suppressor gene product, represses transcription through an interactive nuclear protein. Oncogene **10**:1243-1247.

31. **Scharnhorst, V., P. Dekker, A.J. van der Eb, and A.G. Jochemsen.** 1999. Internal translation initiation generates novel WT1 protein isoforms with distinct biological properties. Journal of Biological Chemistry **274**:23456-23462.

32. **Bruening, W. and J. Pelletier.** 1996. A non-AUG translational initiation event generates novel WT1 isoforms. Journal of Biological Chemistry **271**:8646-8654.

33. **Sharma, P.M., M. Bowman, S.L. Madden, F.J. Rauscher, and S. Sukumar.** 1994. RNA editing in the Wilms' tumor susceptibility gene, WT1. Genes & Development **8**:720-731.

34. **Haber, D.A., R.L. Sohn, A.J. Buckler, J. Pelletier, K.M. Call, and D.E. Housman.** 1991. Alternative splicing and genomic structure of the Wilms

tumor gene WT1. Proceedings of the National Academy of Sciences of the United States of America **88**:9618-9622.

35. **Morris, J.F., S.L. Madden, O.E. Tournay, D.M. Cook, V.P. Sukhatme, and F.J. Rauscher**. 1991. Characterization of the zinc finger protein encoded by the WT1 Wilms' tumor locus. Oncogene **6**:2339-2348.

36. **Wang, Z.Y., Q.Q. Qiu, K.T. Enger, and T.F. Deuel**. 1993. A second transcriptionally active DNA-binding site for the Wilms tumor gene product, WT1. Proceedings of the National Academy of Sciences of the United States of America **90**:8896-8900.

37. **Elser, B., W. Kriz, J.V. Bonventre, C. Englert, and R. Witzgall**. 1997. The Kruppel-associated box (KRAB)-zinc finger protein Kid-1 and the Wilms' tumor protein WT1, two transcriptional repressor proteins, bind to heteroduplex DNA. Journal of Biological Chemistry **272**:27908-27912.

38. **Anant, S., S.A. Axenovich, S.L. Madden, F.J. Rauscher, and K.N. Subramanian**. 1994. Novel replication inhibitory function of the developmental regulator/transcription repressor protein WT1 encoded by the Wilms' tumor gene. Oncogene **9**:3113-3126.

39. **Caricasole, A., A. Duarte, S.H. Larsson, N.D. Hastie, M. Little, G. Holmes, I. Todorov, and A. Ward**. 1996. RNA binding by the Wilms tumor suppressor zinc finger proteins. Proceedings of the National Academy of Sciences of the United States of America **93**:7562-7566.

40. **Bardeesy, N. and J. Pelletier**. 1998. Overlapping RNA and DNA binding domains of the wt1 tumor suppressor gene product. Nucleic Acids Research **26**:1784-1792.

41. **Reddy, J.C. and J.D. Licht**. 1996. The WT1 Wilms' tumor suppressor gene: how much do we really know?. [Review] [201 refs]. Biochimica et Biophysica Acta **1287**:1-28.

42. **Englert, C.** 1998. WT1--more than a transcription factor?. [Review] [53 refs]. Trends in Biochemical Sciences **23**:389-393.

43. **Madden, S.L., D.M. Cook, J.F. Morris, A. Gashler, V.P. Sukhatme, and F.J. Rauscher, III**. 1991. Transcriptional repression mediated by the WT1 Wilms tumor gene product. Science **253**:1550-1553.

44. **Maheswaran, S., S. Park, A. Bernard, J.F. Morris, F.J. Rauscher, D.E. Hill, and D.A. Haber**. 1993. Physical and functional interaction between WT1 and p53 proteins. Proceedings of the National Academy of Sciences of the United States of America **90**:5100-5104.

45. **Englert, C., X. Hou, S. Maheswaran, P. Bennett, C. Ngwu, G.G. Re, A.J. Garvin, M.R. Rosner, and D.A. Haber**. 1995. WT1 suppresses synthesis of the epidermal growth factor receptor and induces apoptosis. EMBO Journal **14**:4662-4675.

46. **Drummond, I.A., S.L. Madden, P. Rohwer-Nutter, G.I. Bell, V.P. Sukhatme, Rauscher, and FJ**. 1992. Repression of the insulin-like growth factor II gene by the Wilms tumor suppressor WT1. Science **257**:674-678.

47. **Gashler, A.L., D.T. Bonthron, S.L. Madden, F.J. Rauscher, T. Collins, Sukhatme, and VP**. 1992. Human platelet-derived growth factor A chain is transcriptionally repressed by the Wilms tumor suppressor WT1. Proceedings of the National Academy of Sciences of the United States of America **89**:10984-10988.

48. **Ryan, G., V. Steele-Perkins, J.F. Morris, F.J. Rauscher, and G.R. Dressler**. 1995. Repression of Pax-2 by WT1 during normal kidney development. Development **121**:867-875.

49. **Rupprecht, H.D., I.A. Drummond, S.L. Madden, F.J. Rauscher, and V.P. Sukhatme**. 1994. The Wilms' tumor suppressor gene WT1 is negatively autoregulated. Journal of Biological Chemistry **269**:6198-6206.

50. **Wang, Z.Y., Q.Q. Qiu, J. Huang, M. Gurrieri, and T.F. Deuel**. 1995. Products of alternatively spliced transcripts of the Wilms' tumor suppressor gene, wt1, have altered DNA binding specificity and regulate transcription in different ways. Oncogene **10**:415-422.

51. **Larsson, S.H., J.P. Charlieu, K. Miyagawa, D. Engelkamp, M. Rassoulzadegan, Ross, F. Cuzin, H. Van, V, and N.D. Hastie**. 1995. Subnuclear localization of WT1 in splicing or transcription factor domains is regulated by alternative splicing. Cell **81**:391-401.

52. **Davies, R.C., C. Calvio, E. Bratt, S.H. Larsson, A.I. Lamond, and N.D. Hastie**. 1998. WT1 interacts with the splicing factor U2AF65 in an isoform-dependent manner and can be incorporated into spliceosomes. Genes & Development **12**:3217-3225.

53. **Klamt, B., A. Koziell, F. Poulat, P. Wieacker, P. Scambler, P. Berta, and Gessler**. 1998. Frasier syndrome is caused by defective alternative splicing of WT1 leading to an altered ratio of WT1 +/-KTS splice isoforms. Human Molecular Genetics **7**:709-714.

54. **Dehbi, M. and J. Pelletier**. 1996. PAX8-mediated activation of the wt1 tumor suppressor gene. EMBO Journal **15**:4297-4306.

55. **Dehbi, M., M. Ghahremani, M. Lechner, G. Dressler, and J. Pelletier**. 1996. The paired-box transcription factor, PAX2, positively modulates

expression of the Wilms' tumor suppressor gene (WT1). Oncogene **13**:447-453.

56. **Cohen, H.T., S.A. Bossone, G. Zhu, G.A. McDonald, and V.P. Sukhatme.** 1997. Sp1 is a critical regulator of the Wilms' tumor-1 gene. Journal of Biological Chemistry **272**:2901-2913.

57. **Torres, M., E. Gomez-Pardo, G.R. Dressler, and P. Gruss.** 1995. Pax-2 controls multiple steps of urogenital development. Development **121**:4057-4065.

58. **Malik, K.T., V. Poirier, S.M. Ivins, and K.W. Brown.** 1994. Autoregulation of the human WT1 gene promoter. FEBS Letters **349**:75-78.

59. **Ye, Y., B. Raychaudhuri, A. Gurney, C.E. Campbell, and B.R. Williams.** 1996. Regulation of WT1 by phosphorylation: inhibition of DNA binding, alteration of transcriptional activity and cellular translocation. EMBO Journal **15**:5606-5615.

60. **Sakamoto, Y., M. Yoshida, K. Semba, and T. Hunter.** 1997. Inhibition of the DNA-binding and transcriptional repression activity of the Wilms' tumor gene product, WT1, by cAMP-dependent protein kinase-mediated phosphorylation of Ser-365 and Ser-393 in the zinc finger domain. Oncogene **15**:2001-2012.

61. **Moffett, P., W. Bruening, H. Nakagama, N. Bardeesy, D. Housman, D.E. Housman, and J. Pelletier.** 1995. Antagonism of WT1 activity by protein self-association. Proceedings of the National Academy of Sciences of the United States of America **92**:11105-11109.

62. **Johnstone, R.W., R.H. See, S.F. Sells, J. Wang, S. Muthukkumar, C. Englert, Haber, DA, J.D. Licht, S.P. Sugrue, T. Roberts, V.M. Rangnekar, and Y. Shi.** 1996. A novel repressor, par-4, modulates transcription and growth suppression functions of the Wilms' tumor suppressor WT1. Molecular & Cellular Biology **16**:6945-6956.

63. **Sells, S.F., D.P.J. Wood, S.S. Joshi-Barve, S. Muthukumar, R.J. Jacob, S.A. Crist, S. Humphreys, and V.M. Rangnekar.** 1994. Commonality of the gene programs induced by effectors of apoptosis in androgen-dependent and -independent prostate cells. Cell Growth & Differentiation **5**:457-466.

64. **Boghaert, E.R., S.F. Sells, A.J. Walid, P. Malone, N.M. Williams, M.H. Weinstein, R. Strange, and V.M. Rangnekar.** 1997. Immunohistochemical analysis of the proapoptotic protein Par-4 in normal rat tissues. Cell Growth & Differentiation **8**:881-890.

65. **Sells, S.F., S.S. Han, S. Muthukkumar, N. Maddiwar, R. Johnstone, E. Boghaert, D. Gillis, G. Liu, P. Nair, S. Monnig, P. Collini, M.P.**

Mattson, V.P. Sukhatme, S.G. Zimmer, D.P.J. Wood, J.W. McRoberts, Y. Shi, and V.M. Rangnekar. 1997. Expression and function of the leucine zipper protein Par-4 in apoptosis. Molecular & Cellular Biology **17**:3823-3832.

66. **Johnstone, R.W., J. Wang, N. Tommerup, H. Vissing, T. Roberts, and Y. Shi**. 1998. Ciao 1 is a novel WD40 protein that interacts with the tumor suppressor protein WT1. Journal of Biological Chemistry **273**:10880-10887.

67. **Neer, E.J., C.J. Schmidt, R. Nambudripad, and T.F. Smith**. 1994. The ancient regulatory-protein family of WD-repeat proteins [published erratum appears in Nature 1994 Oct 27;371(6500):812]. [Review] [68 refs]. Nature **371**:297-300.

68. **van, d., V, Ploegh, and HL**. 1992. The WD-40 repeat. [Review] [27 refs]. FEBS Letters **307**:131-134.

69. **Maheswaran, S., C. Englert, P. Bennett, G. Heinrich, and D.A. Haber**. 1995. The WT1 gene product stabilizes p53 and inhibits p53-mediated apoptosis. Genes & Development **9**:2143-2156.

70. **Donehower, L.A., M. Harvey, B.L. Slagle, M.J. McArthur, C.A.J. Montgomery, J.S. Butel, and A. Bradley**. 1992. Mice deficient for p53 are developmentally normal but susceptible to spontaneous tumours. Nature **356**:215-221.

71. **Scharnhorst, V., P. Dekker, A.J. van der Eb, and A.G. Jochemsen**. 2000. Physical interaction between Wilms tumor 1 and p73 proteins modulates their functions. Journal of Biological Chemistry **275**:10202-10211.

72. **Maheswaran, S., C. Englert, S.B. Lee, R.M. Ezzel, J. Settleman, and D.A. Haber**. 1998. E1B 55K sequesters WT1 along with p53 within a cytoplasmic body in adenovirus-transformed kidney cells. Oncogene **16**:2041-2050.

73. **Kaghad, M., H. Bonnet, A. Yang, L. Creancier, J.C. Biscan, A. Valent, A. Minty, P. Chalon, J.M. Lelias, X. Dumont, P. Ferrara, F. McKeon, and D. Caput**. 1997. Monoallelically expressed gene related to p53 at 1p36, a region frequently deleted in neuroblastoma and other human cancers. Cell **90**:809-819.

74. **Yang, A., M. Kaghad, Y. Wang, E. Gillett, M.D. Fleming, V. Dotsch, N.C. Andrews, D. Caput, and F. McKeon**. 1998. p63, a p53 homolog at 3q27-29, encodes multiple products with transactivating, death-inducing, and dominant-negative activities. Molecular Cell **2**:305-316.

75. **Trink, B., K. Okami, L. Wu, V. Sriuranpong, J. Jen, and D. Sidransky**. 1998. A new human p53 homologue [letter] [see comments] [published erratum appears in Nat Med 1998 Sep;4(9):982]. Nature Medicine **4**:747-748.

76. **Osada, M., M. Ohba, C. Kawahara, C. Ishioka, R. Kanamaru, I. Katoh, Y. Ikawa, Y. Nimura, A. Nakagawara, M. Obinata, and S. Ikawa**. 1998. Cloning and functional analysis of human p51, which structurally and functionally resembles p53 [see comments] [published erratum appears in Nat Med 1998 Sep;4(9):982]. Nature Medicine **4**:839-843.

77. **Schmale, H. and C. Bamberger**. 1997. A novel protein with strong homology to the tumor suppressor p53. Oncogene **15**:1363-1367.

78. **Jost, C.A., M.C. Marin, and W.G. Kaelin, Jr.** 1997. p73 is a simian [correction of human] p53-related protein that can induce apoptosis [see comments] [published erratum appears in Nature 1999 Jun 24;399(6738):817]. Nature **389**:191-194.

79. **Ghebranious, N. and L.A. Donehower**. 1998. Mouse models in tumor suppression. [Review] [243 refs]. Oncogene **17**:3385-3400.

80. **Mills, A.A., B. Zheng, X.J. Wang, H. Vogel, D.R. Roop, and A. Bradley**. 1999. p63 is a p53 homologue required for limb and epidermal morphogenesis. Nature **398**:708-713.

81. **Yang, A., R. Schweitzer, D. Sun, M. Kaghad, N. Walker, R.T. Bronson, C. Tabin, A. Sharpe, D. Caput, C. Crum, and F. McKeon**. 1999. p63 is essential for regenerative proliferation in limb, craniofacial and epithelial development. Nature **398**:714-718.

82. **Zhan, Q., I.T. Chen, M.J. Antinore, and A.J. Fornace, Jr.** 1998. Tumor suppressor p53 can participate in transcriptional induction of the GADD45 promoter in the absence of direct DNA binding [published erratum appears in Mol Cell Biol 1998 Sep;18(9):5620]. Molecular & Cellular Biology **18**:2768-2778.

83. **Kim, J.M., Y. Hong, K. Semba, and S. Kim**. 2000. Physical and functional interaction between the HCMV IE2 protein and the Wilms' tumor suppressor WT1. Biochemical & Biophysical Research Communications **267**:59-63.

84. **Peterson, P.K., H.H.J. Balfour, S.C. Marker, D.S. Fryd, Howard, RJ, and R.L. Simmons**. 1980. Cytomegalovirus disease in renal allograft recipients: a prospective study of the clinical features, risk factors and impact on renal transplantation. Medicine **59**:283-300.

85. **Neiman, P.E., W. Reeves, G. Ray, N. Flournoy, K.G. Lerner, Sale, GE, and E.D. Thomas**. 1977. A prospective analysis interstitial pneumonia and

opportunistic viral infection among recipients of allogeneic bone marrow grafts. Journal of Infectious Diseases **136**:754-767.

86. **Kondo, K. and E.S. Mocarski.** 1995. Cytomegalovirus latency and latency-specific transcription in hematopoietic progenitors. [Review] [24 refs]. Scandinavian Journal of Infectious Diseases - Supplementum **99**:63-67.

87. **Caswell, R., C. Hagemeier, C.J. Chiou, G. Hayward, Kouzarides, and J. Sinclair.** 1993. The human cytomegalovirus 86K immediate early (IE) 2 protein requires the basic region of the TATA-box binding protein (TBP) for binding, and interacts with TBP and transcription factor TFIIB via regions of IE2 required for transcriptional regulation. Journal of General Virology **74**:2691-2698.

88. **Hagemeier, C., R. Caswell, G. Hayhurst, J. Sinclair, and T. Kouzarides.** 1994. Functional interaction between the HCMV IE2 transactivator and the retinoblastoma protein. EMBO Journal **13**:2897-2903.

89. **Speir, E., R. Modali, E.S. Huang, M.B. Leon, F. Shawl, Finkel, and S.E. Epstein.** 1994. Potential role of human cytomegalovirus and p53 interaction in coronary restenosis [see comments]. Science **265**:391-394.

90. **Choi, K.S., S.J. Kim, and S. Kim.** 1995. The retinoblastoma gene product negatively regulates transcriptional activation mediated by the human cytomegalovirus IE2 protein. Virology **208**:450-456.

91. **Yoo, Y.D., C.J. Chiou, K.S. Choi, Y. Yi, S. Michelson, S. Kim, G.S. Hayward, and S.J. Kim.** 1996. The IE2 regulatory protein of human cytomegalovirus induces expression of the human transforming growth factor beta1 gene through an Egr-1 binding site. Journal of Virology **70**:7062-7070.

92. **Ladomery, M.R., J. Slight, G.S. Mc, and N.D. Hastie.** 1999. Presence of WT1, the Wilm's tumor suppressor gene product, in nuclear poly(A)(+) ribonucleoprotein. Journal of Biological Chemistry **274**:36520-36526.

93. **Yitzhaki, S., E. Miriami, R. Sperling, and J. Sperling.** 1996. Phosphorylated Ser/Arg-rich proteins: limiting factors in the assembly of 200S large nuclear ribonucleoprotein particles. Proceedings of the National Academy of Sciences of the United States of America **93**:8830-8835.

94. **Kennedy, D., T. Ramsdale, J. Mattick, and M. Little.** 1996. An RNA recognition motif in Wilms' tumour protein (WT1) revealed by structural modelling. Nature Genetics **12**:329-331.

95. **Zamore, P.D., J.G. Patton, and M.R. Green.** 1992. Cloning and domain structure of the mammalian splicing factor U2AF. Nature **355**:609-614.

96. **Valcarcel, J., R.K. Gaur, R. Singh, and M.R. Green**. 1996. Interaction of U2AF65 RS region with pre-mRNA branch point and promotion of base pairing with U2 snRNA [corrected] [published erratum appears in Science 1996 Oct 4;274(5284):21]. Science **273**:1706-1709.

97. **Wang, Z.Y., Q.Q. Qiu, W. Seufert, T. Taguchi, J.R. Testa, S.A. Whitmore, Callen, DF, D. Welsh, T. Shenk, and T.F. Deuel**. 1996. Molecular cloning of the cDNA and chromosome localization of the gene for human ubiquitin-conjugating enzyme 9. Journal of Biological Chemistry **271**:24811-24816.

98. **Finley, D. and V. Chau**. 1991. Ubiquitination. [Review] [174 refs]. Annual Review of Cell Biology 7:25-69.

99. **Hershko, A. and A. Ciechanover** . 1992. The ubiquitin system for protein degradation. [Review] [216 refs]. Annual Review of Biochemistry **61**:761-807.

100. **Kudoh, T., T. Ishidate, M. Moriyama, K. Toyoshima, and T. Akiyama**. 1995. G1 phase arrest induced by Wilms tumor protein WT1 is abrogated by cyclin/CDK complexes. Proceedings of the National Academy of Sciences of the United States of America **92**:4517-4521.

101. **Maheswaran, S., C. Englert, G. Zheng, S.B. Lee, J. Wong, D.P. Harkin, J. Bean, R. Ezzell, A.J. Garvin, R.T. McCluskey, J.A. DeCaprio, and D.A. Haber**. 1998. Inhibition of cellular proliferation by the Wilms tumor suppressor WT1 requires association with the inducible chaperone Hsp70. Genes & Development **12**:1108-1120.

102. **Khanna, A., R.F. Aten, and H.R. Behrman**. 1995. Heat shock protein-70 induction mediates luteal regression in the rat. Molecular Endocrinology **9**:1431-1440.

103. **Leppa, S., L. Pirkkala, H. Saarento, K.D. Sarge, and L. Sistonen**. 1997. Overexpression of HSF2-beta inhibits hemin-induced heat shock gene expression and erythroid differentiation in K562 cells. Journal of Biological Chemistry **272**:15293-15298.

104. **Creighton, T.E.** 1991. Molecular chaperones. Unfolding protein folding [news; comment] [see comments]. Nature **352**:17-18.

105. **Hartl, F.U.** 1996. Molecular chaperones in cellular protein folding. [Review] [154 refs]. Nature **381**:571-579.

106. **Lindquist, S. and E.A. Craig**. 1988. The heat-shock proteins. [Review] [259 refs]. Annual Review of Genetics **22**:631-677.

107. **Milarski, K.L. and R.I. Morimoto.** 1989. Mutational analysis of the human HSP70 protein: distinct domains for nucleolar localization and adenosine triphosphate binding. Journal of Cell Biology **109**:1947-1962.

108. **Wu, B.J. and R.I. Morimoto.** 1985. Transcription of the human hsp70 gene is induced by serum stimulation. Proceedings of the National Academy of Sciences of the United States of America **82**:6070-6074.

109. **Kingston, R.E., A.S.J. Baldwin, and P.A. Sharp.** 1984. Regulation of heat shock protein 70 gene expression by c-myc. Nature **312**:280-282.

110. **Kao, H.T. and J.R. Nevins.** 1983. Transcriptional activation and subsequent control of the human heat shock gene during adenovirus infection. Molecular & Cellular Biology **3**:2058-2065.

111. **Khandjian, E.W. and H. Turler** . 1983. Simian virus 40 and polyoma virus induce synthesis of heat shock proteins in permissive cells. Molecular & Cellular Biology **3** :1-8.

112. **Nachtigal, M.W., Y. Hirokawa, D.L. Enyeart-VanHouten, J.N. Flanagan, G.D. Hammer, and H.A. Ingraham.** 1998. Wilms' tumor 1 and Dax-1 modulate the orphan nuclear receptor SF-1 in sex-specific gene expression. Cell **93**:445-454.

113. **Lala, D.S., D.A. Rice, and K.L. Parker.** 1992. Steroidogenic factor I, a key regulator of steroidogenic enzyme expression, is the mouse homolog of fushi tarazu-factor I. Molecular Endocrinology **6**:1249-1258.

114. **Morohashi, K.** 1998. [Function and expression of transcription factors implicated in gonadal differentiation]. [Review] [19 refs] [Japanese]. Nippon Rinsho - Japanese Journal of Clinical Medicine **56**:1739-1744.

115. **Luo, X., Y. Ikeda, and K.L. Parker.** 1994. A cell-specific nuclear receptor is essential for adrenal and gonadal development and sexual differentiation. Cell **77**:481-490.

116. **Parker, K.L., A. Schedl, and B.P. Schimmer.** 1999. Gene interactions in gonadal development. [Review] [95 refs]. Annual Review of Physiology **61**:417-433.

117. **Swain, A. and R. Lovell-Badge** . 1997. A molecular approach to sex determination in mammals. [Review] [29 refs]. Acta Paediatrica **Supplement. 423**:46-49.

118. **Kim, J., K. Lee, and J. Pelletier.** 1998. The DNA binding domains of the WT1 tumor suppressor gene product and chimeric EWS/WT1 oncoprotein are functionally distinct. Oncogene **16**:1021-1030.

119. **Sambrook, J., E.F. Fritsch, and T. Maniatis**. 1989. Molecular Cloning: a laboratory manual. Cold Spring Harbor Laboratory,

120. **Friedman, J.R., W.J. Fredericks, D.E. Jensen, D.W. Speicher, X.P. Huang, E.G. Neilson, and F.J. Rauscher**. 1996. KAP-1, a novel corepressor for the highly conserved KRAB repression domain. Genes & Development **10**:2067-2078.

121. **Han, Z.G., Q.H. Zhang, M. Ye, L.X. Kan, B.W. Gu, K.L. He, S.L. Shi, J. Zhou, G. Fu, M. Mao, S.J. Chen, L. Yu, and Z. Chen**. 1999. Molecular cloning of six novel Kruppel-like zinc finger genes from hematopoietic cells and identification of a novel transregulatory domain KRNB. Journal of Biological Chemistry **274**:35741-35748.

122. **Sanger, F., S. Nicklen, and A.R. Coulson**. 1977. DNA sequencing with chain-terminating inhibitors. Proceedings of the National Academy of Sciences of the United States of America **74**:5463-5467.

123. **Jurata, L.W. and G.N. Gill**. 1998. Structure and function of LIM domains. [Review] [148 refs]. Current Topics in Microbiology & Immunology **228**:75-113.

124. **Shawlot, W. and R.R. Behringer**. 1995. Requirement for Lim1 in head-organizer function [see comments]. Nature **374**:425-430.

125. **Warren, A.J., W.H. Colledge, M.B. Carlton, M.J. Evans, A.J. Smith, and T.H. Rabbitts**. 1994. The oncogenic cysteine-rich LIM domain protein rbtn2 is essential for erythroid development. Cell **78**:45-57.

126. **Ono, Y., T. Fujii, K. Igarashi, T. Kuno, C. Tanaka, Kikkawa, and Y. Nishizuka**. 1989. Phorbol ester binding to protein kinase C requires a cysteine-rich zinc-finger-like sequence. Proceedings of the National Academy of Sciences of the United States of America **86**:4868-4871.

127. **Mott, H.R., J.W. Carpenter, S. Zhong, S. Ghosh, R.M. Bell, and S.L. Campbell**. 1996. The solution structure of the Raf-1 cysteine-rich domain: a novel ras and phospholipid binding site. Proceedings of the National Academy of Sciences of the United States of America **93**:8312-8317.

128. **Falquet, L., N. Paquet, S. Frutiger, G.J. Hughes, K. Hoang-Van, and J.C. Jaton**. 1995. cDNA cloning of a human 100 kDa de-ubiquitinating enzyme: the 100 kDa human de-ubiquitinase belongs to the ubiquitin C-terminal hydrolase family 2 (UCH2). FEBS Letters **376**:233-237.

129. **Grozinger, C.M., C.A. Hassig, and S.L. Schreiber**. 1999. Three proteins define a class of human histone deacetylases related to yeast Hda1p. Proceedings of the National Academy of Sciences of the United States of America **96**:4868-4873.

130. www.ncbi.nlm.nih.gov/Genbank/genbankstats.html . 8-8-2000. (GENERIC) Ref Type: Electronic Citation

131. **Jacobs, G.H.** 1992. Determination of the base recognition positions of zinc fingers from sequence analysis. EMBO Journal **11**:4507-4517.

132. **MacKay, J.P. and M. Crossley**. 1998. Zinc fingers are sticking together. [Review] [37 refs]. Trends in Biochemical Sciences **23**:1-4.

133. **Georgopoulos, K., S. Winandy, and N. Avitahl**. 1997. The role of the Ikaros gene in lymphocyte development and homeostasis. [Review] [51 refs]. Annual Review of Immunology **15**:155-176.

134. **Morgan, B., L. Sun, N. Avitahl, K. Andrikopoulos, T. Ikeda, E. Gonzales, P. Wu, S. Neben, and K. Georgopoulos** . 1997. Aiolos, a lymphoid restricted transcription factor that interacts with Ikaros to regulate lymphocyte differentiation. EMBO Journal **16**:2004-2013.

135. **Tsang, A.P., J.E. Visvader, C.A. Turner, Y. Fujiwara, C. Yu, M.J. Weiss, M. Crossley, and S.H. Orkin**. 1997. FOG, a multitype zinc finger protein, acts as a cofactor for transcription factor GATA-1 in erythroid and megakaryocytic differentiation. Cell **90**:109-119.

136. **Omichinski, J.G., P.V. Pedone, G. Felsenfeld, A.M. Gronenborn, and G.M. Clore**. 1997. The solution structure of a specific GAGA factor-DNA complex reveals a modular binding mode [see comments]. Nature Structural Biology **4**:122-132.

137. **Merika, M. and S.H. Orkin**. 1995. Functional synergy and physical interactions of the erythroid transcription factor GATA-1 with the Kruppel family proteins Sp1 and EKLF. Molecular & Cellular Biology **15**:2437-2447.

138. **Crossley, M., M. Merika, and S.H. Orkin**. 1995. Self-association of the erythroid transcription factor GATA-1 mediated by its zinc finger domains. Molecular & Cellular Biology **15**:2448-2456.

139. **Inoue, K., H. Sugiyama, H. Ogawa, M. Nakagawa, T. Yamagami, H. Miwa, K. Kita, A. Hiraoka, T. Masaoka, and K. Nasu**. 1994. WT1 as a new prognostic factor and a new marker for the detection of minimal residual disease in acute leukemia. Blood **84**:3071-3079.

140. **Miyagi, T., H. Ahuja, T. Kubota, I. Kubonishi, H.P. Koeffler, and I. Miyoshi**. 1993. Expression of the candidate Wilm's tumor gene, WT1, in human leukemia cells. Leukemia **7**:970-977.

141. **Miwa, H., M. Beran, and G.F. Saunders**. 1992. Expression of the Wilms' tumor gene (WT1) in human leukemias. Leukemia **6**:405-409.

142. **Oka, Y., K. Udaka, A. Tsuboi, O.A. Elisseeva, H. Ogawa, K. Aozasa, T. Kishimoto, and H. Sugiyama**. 2000. Cancer immunotherapy targeting Wilms' tumor gene WT1 product. Journal of Immunology **164**:1873-1880.

143. **Hirose, M.** 1999. The role of Wilms' tumor genes. [Review] [82 refs]. Journal of Medical Investigation **46**:130-140.

144. **Smith, S.I., M. Down, A.W. Boyd, and C.L. Li**. 2000. Expression of the Wilms' tumor suppressor gene, WT1, reduces the tumorigenicity of the leukemic cell line M1 in C.B-17 scid/scid mice. Cancer Research **60**:808-814.

145. **Williams, A.J., S.C. Blacklow, and T. Collins**. 1999. The zinc finger-associated SCAN box is a conserved oligomerization domain. Molecular & Cellular Biology **19**:8526-8535.

146. **Perkins, A.C., A.H. Sharpe, and S.H. Orkin**. 1995. Lethal beta-thalassaemia in mice lacking the erythroid CACCC-transcription factor EKLF. Nature **375**:318-322.

147. **Nuez, B., D. Michalovich, A. Bygrave, R. Ploemacher, and F. Grosveld**. 1995. Defective haematopoiesis in fetal liver resulting from inactivation of the EKLF gene. Nature **375**:316-318.

148. **van Ree, J.H., M.A. Roskrow, A.M. Becher, R. McNall, V.A. Valentine, S.M. Jane, and J.M. Cunningham**. 1997. The human erythroid-specific transcription factor EKLF localizes to chromosome 19p13.12-p13.13. Genomics **39**:393-395.

149. **Olopade, O.I., M. Thangavelu, R.A. Larson, R. Mick, V. Kowal, H.R. Schumacher, M.M. Le Beau, J.W. Vardiman, and J.D. Rowley**. 1992. Clinical, morphologic, and cytogenetic characteristics of 26 patients with acute erythroblastic leukemia. Blood **80**:2873-2882.